The Instantaneous Spectrum: A General Framework for Time-Frequency Analysis

Steven Sandoval, *Member, IEEE,* Phillip L. De Leon, *Senior Member, IEEE*

***Abstract*—This paper is a contribution to the old problem of representing a signal in the coordinates of time and frequency. We review the fundamental Hilbert transform relationship in systems analysis and argue that the dual relationship assumed in signal analysis, i.e. spectral single-sidedness is not necessarily justifiable. Therefore, we abandon the analytic signal and utilize a carefully parameterized signal model composed of a superposition of complex, AM–FM components that enables rigorous definition of instantaneous amplitude and instantaneous frequency. We then propose the instantaneous spectrum (IS) and prove that it exactly localizes signal components in an instantaneous bandwidth sense. The relation of the IS to traditional time-frequency distributions is discussed and comparative examples are provided. It is shown that under certain conditions the IS specializes to the Fourier spectrum and properties of the IS, similar to standard Fourier transform properties, are given.**

***Index Terms*—Signal analysis, Spectral analysis.**

I. Introduction

CLASSICALLY, description of a signal consists of two complementary views, that of the *time* and *frequency* domains [1]–[3]. By *time*, we refer to the value of the signal as a function of time and by *frequency* we refer to the *spectrum* of the signal as a function of frequency, determined by the Fourier transform (FT). Historically, the notion of *generalized frequency* was introduced around the dawn of FM communications [4]–[6] and *generalized spectra* became of interest around the dawn of the spectrograph [7]. Specifically, Carson proposed [5] a generalization of frequency termed *instantaneous frequency* (IF) and Gabor proposed [7] a framework for joint time-frequency analysis (TFA) leading to the formal study of *time-frequency distributions* (TFDs).

TFDs do not fully generalize the notion of frequency as per Carson. Rather, using the Hilbert transform (HT) and the so-called "analytic signal" (AS) also introduced by Gabor [7], Ville *speciously* combined Carson's notion of generalized frequency, with Gabor's notion of generalized spectra [8]. Hitherto, nearly all modern TFA methods build upon these foundations [9]–[14]. Unfortunately, while unquestionably mathematically correct, these foundations only present one of the possible perspectives one may take in framing the TFA problem (see Fig. 1) because generalized frequency is not utilized in the broadest way possible. Although Gabor was aware of Carson's generalization, he erroneously notes [7] that Carson's concept of IF "...is a useful notion for slowly-varying frequencies, but not sufficient to cover all cases...." Our position, is that in fact, it is Gabor's framework which is not sufficient for IF.

In this paper, we re-evaluate fundamental principles of TFA by returning to first principles, then develop the concept of an instantaneous spectrum (IS), in which the notion of generalized frequency, as proposed by Carson, is utilized to the fullest extent. Traditional TFD research has evolved to describe a problem in which we seek a function that describes the *energy* of the signal simultaneously in time and frequency and where mathematical manipulation may be performed in the same way as with probability distributions and densities [10]. On the contrary, we propose an alternative TFA where the problem is to find a set of parameters that will map to both an instantaneous time-frequency *spectrum* and a *signal*, and where the mathematical description is similar to a coordinate system. Unlike previous attempts to define an IS, we believe that ties with the FT and HT, in general, must be severed and maintained only in special cases. In contrast to TFDs which require at a minimum one FT and often one HT, our formulation does not, in general, require the use of the FT or HT. This leads to a generalized framework for TFA.

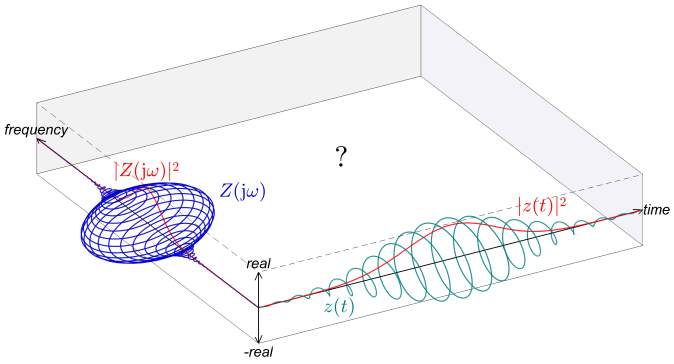

Figure 1. Illustration of the time-frequency analysis problem. Classical analysis consists of two complementary views: the time domain and the frequency domain. A complex-valued signal $z(t)$ (—) and its instantaneous power $|z(t)|^2$ (—) are illustrated along the time axis and the corresponding complex-valued Fourier spectrum $Z(\mathrm{j}\omega)$ (—) and its energy density $|Z(\mathrm{j}\omega)|^2$ (—) are illustrated along the frequency axis. Placing the time and frequency axes orthogonal to each other (overloading the time, frequency, and imaginary dimensions to allow visualization of four dimensions), the question may be asked: *How does one mathematically describe a signal as a function not of t and ω separately, but rather, simultaneously in the space they span?*

This paper has supplementary downloadable material available at http://ieeexplore.ieee.org, provided by the authors. This includes an animation and all figures in the paper. This material is 85 MB in size.

The authors are with Klipsch School of Electrical and Computer Engineering, New Mexico State University (NMSU), Las Cruces NM 88003 USA. e-mail: {spsandov, pdeleon}@nmsu.edu **(Accepted: 27 Aug. 2018)**

This paper and our contributions are organized as follows. In Section II, we provide an original argument that the assumption of spectral single-sidedness is not fundamental for signal analysis and in Section III, we briefly review IF noting that the commonly-accepted definition of IF for a real signal only holds for a limited class of signals. In Sections IV and V, we utilize a carefully parameterized signal model based on complex AM–FM components which ultimately leads to a general and rigorous approach for parameterizing and representing a signal. In Section VI, we propose a new view of signals and argue the importance of choosing the imaginary signal part in the most general way possible in order to fully utilize the components. The key theoretical results and the main contributions of this work are presented in Section VII where we build upon the prior sections in order to define a generalized spectrum and provide associated properties. We point out that the IS may be considered as the ideal Dirac-type time-frequency representation (TFR) and prove that with the complex AM–FM model and corresponding IS, *exact localization in time and frequency is inherent*. In Section VIII, we provide comparative examples with TFDs. Finally, in Sections IX and X we provide a short discussion and conclusions.

II. Hilbert Transform and the Analytic Signal

Although the HT is considered by some to be the most important operator in mathematical analysis [15], the applicability in engineering practice is often misunderstood [16]. In Lee and Wiener's work in the 1930s, the fundamental HT relationship between the real and imaginary parts of the immittance function was discovered [16]. The relationship can be shown as follows [17]. Let the real impulse response of a system be expressed in terms of even and odd parts $h(t) = h_{\mathrm{e}}(t) + h_{\mathrm{o}}(t)$. If the system is causal, this implies $h_{\mathrm{o}}(t) = \operatorname{sgn}(t) h_{\mathrm{e}}(t)$ where $\operatorname{sgn}(\cdot)$ denotes the sign function and the frequency response is $H(\mathrm{j}\omega) = H_{\mathrm{R}}(\mathrm{j}\omega) + \mathrm{j}H_{\mathrm{I}}(\mathrm{j}\omega)$ where $H_{\mathrm{R}}(\mathrm{j}\omega)$ and $H_{\mathrm{I}}(\mathrm{j}\omega)$ denote the real and imaginary parts. Therefore,

$$\begin{array}{ccccc} h_{\mathrm{o}}(t) & = \operatorname{sgn}(t) & \times & h_{\mathrm{e}}(t) \\ \updownarrow \mathcal{F} & & \updownarrow \mathcal{F} & & \updownarrow \mathcal{F} \\ \mathrm{j}H_{\mathrm{I}}(\mathrm{j}\omega) = & \dfrac{\mathrm{j}}{\pi\omega} & \underset{\text{p.v.}}{*} & H_{\mathrm{R}}(\mathrm{j}\omega) \end{array}$$

where the lower line may be re-written as

$$H_{\mathrm{I}}(\mathrm{j}\omega) = \mathcal{H}\{H_{\mathrm{R}}(\mathrm{j}\omega)\} \triangleq \frac{1}{\pi} \fint_{-\infty}^{\infty} \frac{H_{\mathrm{R}}(\mathrm{j}\omega)}{\omega - \omega} \, \mathrm{d}\omega$$

where $\underset{\text{p.v.}}{*}$ and $\fint$ denote the Cauchy principle value of convolution and integration due to the singularity [1], $\mathcal{H}\{\cdot\}$ denotes the HT operator, and $\overset{\mathcal{F}}{\longleftrightarrow}$ denotes a FT pair. This relationship allows one to determine, for example, the group delay $-\frac{\mathrm{d}}{\mathrm{d}\omega}\angle H(\mathrm{j}\omega)$ from a *measurable* frequency response $H_{\mathrm{R}}(\mathrm{j}\omega)$ of a causal *system* without actually measuring $H_{\mathrm{I}}(\mathrm{j}\omega)$.

Consider the dual form of the above, but for a *general signal*: express the complex frequency spectrum for a signal $z(t) = x(t) + \mathrm{j}y(t)$ in terms of conjugate symmetries as $Z(\mathrm{j}\omega) = Z_{\mathrm{cs}}(\mathrm{j}\omega) + Z_{\mathrm{ca}}(\mathrm{j}\omega)$ with conjugate symmetric part $Z_{\mathrm{cs}}(\mathrm{j}\omega) = X(\mathrm{j}\omega) \overset{\mathcal{F}}{\longleftrightarrow} x(t)$ and conjugate anti-symmetric part $Z_{\mathrm{ca}}(\mathrm{j}\omega) = \mathrm{j}Y(\mathrm{j}\omega) \overset{\mathcal{F}}{\longleftrightarrow} \mathrm{j}y(t)$ where both $x(t)$ and $y(t)$ are real-valued and both $X(\mathrm{j}\omega)$ and $Y(\mathrm{j}\omega)$ are complex-valued. If we assume the frequency spectrum is zero for negative frequencies, this implies $Z_{\mathrm{ca}}(\mathrm{j}\omega) = \operatorname{sgn}(\omega) Z_{\mathrm{cs}}(\mathrm{j}\omega)$, then we write $Z(\mathrm{j}\omega) \to Z_{\mathsf{a}}(\mathrm{j}\omega)$, $z(t) \to z_{\mathsf{a}}(t)$, $y(t) \to y_{\mathsf{a}}(t)$, where subscript a stands for analytic and it follows that

$$\begin{array}{ccccc} Z_{\mathrm{ca}}(\mathrm{j}\omega) & = \operatorname{sgn}(\omega) & \times & Z_{\mathrm{cs}}(\mathrm{j}\omega) \\ \updownarrow \mathcal{F} & & \updownarrow \mathcal{F} & & \updownarrow \mathcal{F} \\ \mathrm{j}y_{\mathsf{a}}(t) & = \dfrac{\mathrm{j}}{\pi t} & \underset{\text{p.v.}}{*} & x(t) \end{array}$$

where the lower line may be re-written as

$$y_{\mathsf{a}}(t) \triangleq \mathcal{H}\{x(t)\} \triangleq \frac{1}{\pi} \fint_{-\infty}^{\infty} \frac{x(\tau)}{\tau - t} \, \mathrm{d}\tau$$

and the so-called AS is defined as

$$z_{\mathsf{a}}(t) \triangleq x(t) + \mathrm{j}y_{\mathsf{a}}(t). \tag{1}$$

This allows one to determine $z_{\mathsf{a}}(t)$ from a measurable $x(t)$ without actually measuring $y(t)$. Furthermore, expressing in polar form $z_{\mathsf{a}}(t) = \rho_{\mathsf{a}}(t) \mathrm{e}^{\mathrm{j}\Theta_{\mathsf{a}}(t)}$ where $\rho_{\mathsf{a}}(t)$ is the instantaneous amplitude (IA), $\Theta_{\mathsf{a}}(t)$ is the phase, and $\frac{\mathrm{d}}{\mathrm{d}t}\Theta_{\mathsf{a}}(t)$ is the IF [5]. This is exactly the procedure advocated by Ville [8], following the seminal work by Gabor [7]. Unfortunately, while a causality assumption for *system analysis* is physically justifiable, an assumption of spectral single-sidedness is not necessarily justifiable for *signal analysis*. In other words, the HT relationship is fundamental in causal system analysis [16], but no such fundamental relationship in signal analysis exists. This is in contrast to the work of Vakman [18]–[22], who argued spectral single-sidedness is justifiable for signal analysis through mathematical constraints he believed to be physically-justified: (a) amplitude continuity, (b) phase independence on scale changes and homogeneity, (c) harmonic correspondence (HC), and (d) phase continuity. With these constraints, in particular HC[1], Vakman argued that the imaginary part of the AS $z_{\mathsf{a}}(t)$, $y_{\mathsf{a}}(t) = \mathcal{H}\{x(t)\}$ is fundamental in signal analysis. On the other hand, we believe that HC is overly restrictive.

Consider a system in which the output satisfies the differential equation describing simple harmonic motion

$$\frac{\mathrm{d}^2}{\mathrm{d}t^2} z(t) + {\omega_0}^2 z(t) = 0 \tag{2}$$

where it is assumed the output of the system $z(t)$ is complex and the real part is measured as $x(t) = \alpha \cos(\omega_0 t + \phi)$. The problem is to determine $y(t)$ such that $z(t) = x(t) + \mathrm{j}y(t)$ satisfies (2). One solution is given by

$$z_{\mathsf{a}}(t) = \alpha \mathrm{e}^{\mathrm{j}(\omega_0 t + \phi)}$$

where HC implies $y(t) = \alpha \sin(\omega_0 t + \phi) = \mathcal{H}\{x(t)\}$ [23]. This solution is spectrally single-sided and thus appears to tie spectral single-sidedness to a physically-motivated differential equation. However, for the same measurement $x(t)$

$$z(t) = \alpha \cos(\omega_0 t + \phi) + \mathrm{j}\beta \sin(\omega_0 t + \phi) \tag{3a}$$

$$= \frac{1}{2}(\alpha + \beta) \mathrm{e}^{\mathrm{j}(\omega_0 t + \phi)} + \frac{1}{2}(\alpha - \beta) \mathrm{e}^{-\mathrm{j}(\omega_0 t + \phi)} \tag{3b}$$

[1]Let $x(t) = a_0 \cos(\omega_0 t + \phi_0)$, then HC forces $z(t) = a_0 \mathrm{e}^{\mathrm{j}(\omega_0 t + \phi_0)}$ [22].

also satisfies (2) and most importantly, the spectrum of (3) is not single-sided. Therefore, HC is not a fundamental signal property and by avoiding the general use of the AS, will not be imposed in the following sections.

III. Instantaneous Frequency

In 1937, Carson and Fry formally defined a generalized notion of frequency, termed IF, based on the phase derivative of a complex signal [5], [6]. In 1947, Gabor proposed the AS as a complex extension of a real signal [7]. Ville used Gabor's AS and Carson's IF definition to define the IF of a real signal [23]. Using the AS to extend Carson's IF definition for a real signal, results in a number of useful relationships. As a result, the AS is almost universally viewed as the correct way to define the complex signal from the real signal and subsequently, the correct way to define IA, IF, and phase for real signals despite the inherent assumption of HC in the AS.

Historically, the concept of IF in engineering literature has been controversial [24]–[26] and several so-called paradoxes have been brought to attention [10], [22]. The commonly accepted definition of IF for a real signal as the derivative of the phase function of the AS, only holds for a limited class of signals [8], [10]. The problem with the AS approach was pointed out by Shekel in [24]. As an example, consider

$$x(t) = \operatorname{Re}\Big\{ a(t) \mathrm{e}^{\mathrm{j}\left[\int_{-\infty}^{t} \omega(\tau)\,\mathrm{d}\tau + \phi\right]} \Big\}$$

where $\operatorname{Re}\{\cdot\}$ denotes the real operator. There is an infinite set of pairs of $a(t)$ and $\omega(t)$ for which $x(t)$ may be equivalently described and hence an infinite set of IA/IF parameterizations.

Although Carson's definition of IF as the phase derivative of a complex signal is without question, the HT relation is not fundamental in signal analysis, and consequently, Gabor's AS approach is not necessarily the appropriate way to complex extend a real signal for purposes of determining the IA/IF. This leads to the problem we term, *complex extension* and is discussed in further detail in Section VI.

IV. The Complex AM–FM Component

In order to *exhaustively* use the concept of IF in signal analysis, we must define the *most general* signal component which is compatible with Carson's IF definition. At present, there is no clear agreed-upon definition of a component or a monocomponent signal in the time-frequency literature [10], [23], [27]. Therefore, we propose to define a complex AM–FM component as any signal that may be expressed using only a single IA and single IF. Thus, in the most general sense, a complex AM–FM component is any complex-valued signal that can be expressed as

$$\psi\big(t;\mathscr{C}\big) \triangleq a(t) \exp\left(\mathrm{j} \left[\int_{-\infty}^{t} \omega(\tau)\,\mathrm{d}\tau + \phi \right] \right) \tag{4}$$

where $\mathscr{C} \triangleq \big(a(t), \omega(t), \phi\big)$ is a canonical triplet. This definition is useful because it guarantees differentiability of the phase function, ensuring both a well-defined IA and IF.

Similar to the work of Picinbono [28], who used canonical pairs for signal parameterization, the AM–FM component is parameterized by $\mathscr{C}$. Importantly, this parameterization will subsequently be interpreted as a type of coordinate system, i.e. rather than expressing the signal component in terms of a Cartesian canonical pair consisting of real and imaginary parts $\big(s(t), \sigma(t)\big)$ or a polar canonical pair consisting of amplitude and angle $\big(a(t), \theta(t)\big)$, we express in terms of an AM–FM canonical triplet consisting of amplitude, angular velocity, and an angle reference $\big(a(t), \omega(t), \phi\big)$. We use this analogy to develop a coordinate system for TFA.

In general, a signal requires multiple IAs and IFs for a meaningful description, thus requiring a decomposition into multiple complex AM–FM components [23], [29]; a multicomponent signal model will be discussed next. Additionally, in practice only a real-valued signal is measurable, however, a complex-valued signal is required for determining the IA and IF. This complex extension problem will be discussed in Section VI.

V. The Complex AM–FM Model

We meticulously parameterize the complex AM–FM model for a complex signal $z(t)$ as a superposition of K (possibly infinite) complex AM–FM components

$$\begin{aligned} z\big(t;\mathscr{S}\big) &\triangleq \sum_{k=0}^{K-1} \psi_k\big(t;\mathscr{C}_k\big) && \text{(5a)} \\ &= \rho(t) \mathrm{e}^{\mathrm{j}\left[\int_{-\infty}^{t} \Omega(\tau)\,\mathrm{d}\tau + \Phi\right]} && \text{(5b)} \\ &= \rho(t) \mathrm{e}^{\mathrm{j}\Theta(t)} && \text{(5c)} \\ &= x(t) + \mathrm{j}y(t) && \text{(5d)} \end{aligned}$$

where $\mathscr{S} \triangleq \{\mathscr{C}_0, \mathscr{C}_1, \cdots, \mathscr{C}_{K-1}\}$ is the component set; $\mathscr{C}_k \triangleq \big(a_k(t), \omega_k(t), \phi_k\big)$ is the canonical triplet for the kth component; and for the signal $z(t)$, $\rho(t)$ is the IA, $\Theta(t)$ is the phase function, $\Omega(t) = \frac{\mathrm{d}}{\mathrm{d}t}\Theta(t)$ is the IF, Φ is the phase reference, $x(t)$ is the real part, and $y(t)$ is the imaginary part. The kth complex AM–FM component in (5a) is defined as

$$\begin{aligned} \psi_k\big(t;\mathscr{C}_k\big) &\triangleq a_k(t) \mathrm{e}^{\mathrm{j}\left[\int_{-\infty}^{t} \omega_k(\tau)\,\mathrm{d}\tau + \phi_k\right]} && \text{(6a)} \\ &= a_k(t) \mathrm{e}^{\mathrm{j}\theta_k(t)} && \text{(6b)} \\ &= s_k(t) + \mathrm{j}\sigma_k(t) && \text{(6c)} \end{aligned}$$

where for the kth AM–FM component $\psi_k(t)$, $a_k(t)$ is the IA, $\theta_k(t)$ is the phase function,

$$\omega_k(t) = \frac{\mathrm{d}}{\mathrm{d}t}\theta_k(t) \tag{7}$$

is the IF, ϕ_k is the phase reference, $s_k(t)$ is the real part, and $\sigma_k(t)$ is the imaginary part. Rewriting $\omega_k(t) = \varpi_k + m_k(t)$, the phase $\theta_k(t)$ may be expressed in terms of frequency reference ϖ_k and FM message $m_k(t)$ as $\theta_k(t) = \varpi_k t + \int_{-\infty}^{t} m_k(\tau)\,\mathrm{d}\tau + \phi_k$ or in terms of the phase modulation message $M_k(t)$ as $\theta_k(t) = \varpi_k t + M_k(t) + \phi_k$. The geometric interpretations of the AM–FM component in (4) and the AM–FM model in (5) are illustrated with the Argand diagrams in Fig. 2. The AM–FM component can be visually interpreted as a single rotating vector in the complex plane with time-varying length and time-varying angular velocity. The time evolution of the AM–FM model may be interpreted directly in terms of

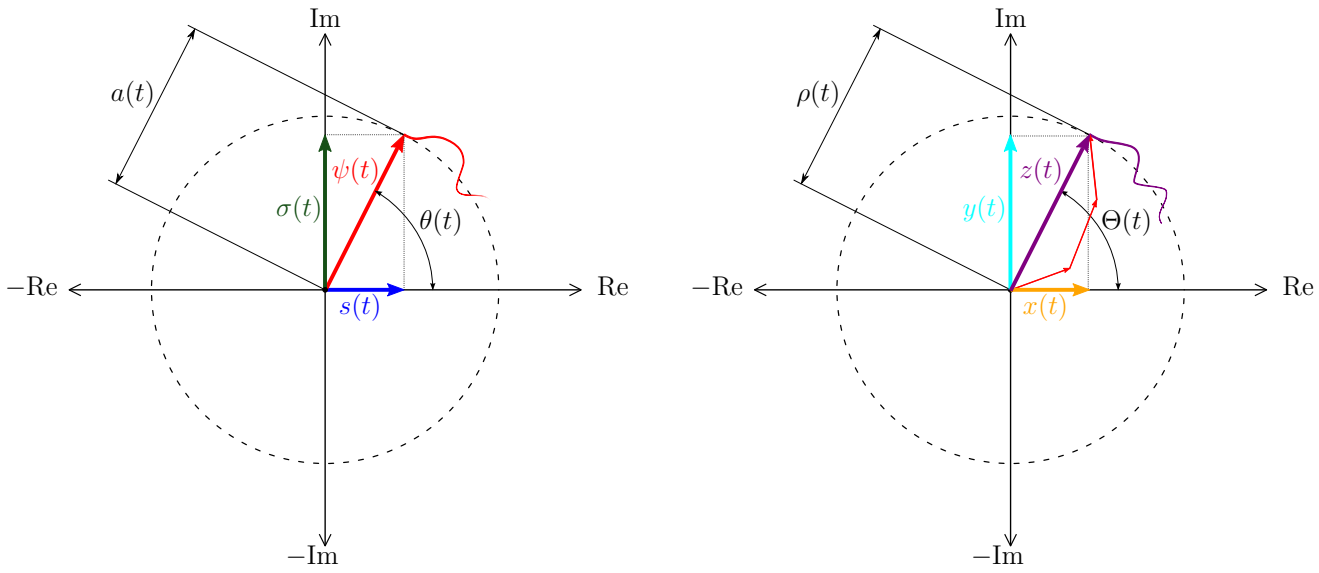

Figure 2. (a) Argand diagram of an AM–FM component in (4) at some time instant. Each component, $\psi(t)$ (⟶) is interpreted as a vector: the IA $a(t)$ (↤↦) is interpreted as the component vector's length, the phase $\theta(t)$ (↶) is interpreted as a component vectors's angular position. Although not shown, the IF $\omega(t)$ is interpreted as a component vector's angular velocity and phase reference ϕ is interpreted as the angular position at $t = 0$. The real part of the component $s(t)$ (⟶) and the imaginary part of the component $\sigma(t)$ (⟶) are interpreted as orthogonal projections of $\psi(t)$. We have included an example path (—) taken by $\psi(t)$. (b) Argand diagram of the signal $z(t)$ (⟶) in (5) at some time instant, composed of a superposition of components (⟶). The signal is interpreted as a vector: the IA $\rho(t)$ (↤↦) is interpreted as the signal vector's length, the phase $\Theta(t)$ (↶) is interpreted as a signal vector's angular position, and although not shown the IF $\Omega(t)$ is interpreted as a signal vector's angular velocity. The real part of the signal $x(t)$ (⟶) and the imaginary part of the signal $y(t)$ (⟶) are interpreted as orthogonal projections of $z(t)$. We have included an example path (—) taken by $z(t)$.

mechanics—where the sometimes misunderstood concept of IF [25] may be conveniently interpreted as angular velocity.

We assume that the phase and frequency references are selected at $t = 0$, i.e. $\int_{-\infty}^{0} \omega_k(t)\,\mathrm{d}t = 0$ which implies $\int_{-\infty}^{0} m_k(t)\,\mathrm{d}t = M_k(0) = 0$, $\phi_k = \theta_k(0)$, and $\varpi_k = \omega_k(0) - m_k(0)$. We define a *monocomponent signal* as any signal expressed with $K = 1$ and thus with a single canonical triplet. A *multicomponent signal* can then be defined as any signal expressed with $K > 1$ and thus with a set of canonical triplets. This definition is useful because it allows a great amount of flexibility in the signal model while also parameterizing the signal in a useful way. We emphasize that our use of the complex AM–FM model is specifically to allow a rigorous parameterization. In contrast, traditional AM–FM models in literature, typically refer to specific computational methods for finding a set of parameters under a specific set of constraints. A brief review of computational AM–FM models is provided in Appendix A.

VI. Latent Signal Analysis

The complex-valued nature of the proposed model leads to a new, possibly radical view of signals. This view is that all signals are in fact complex-valued and that in reality, only the real part $x(t)$, is observed (or measured) and the imaginary part $y(t)$, is *latent*, i.e. the act of observation corresponds to

$$z(t) \mapsto x(t) \quad \text{according to} \quad x(t) = \mathrm{Re}\{z(t)\}. \tag{8}$$

We term this view Latent Signal Analysis (LSA). The problem considered in LSA is to determine a complex signal extension, i.e. to determine the (total) *latent signal* $z(t) = x(t) + \mathrm{j}y(t)$ when the imaginary part $y(t)$ is hidden, given an observation $x(t)$. This is analogous to Lee's problem [16] in determining $H(\mathrm{j}\omega)$ from the real measurement $H_{\mathrm{R}}(\mathrm{j}\omega)$.

Traditionally, there are two choices for $y(t)$ that are made in the literature. If one chooses $y(t) = 0$, then conjugate symmetry is imposed in frequency, i.e. $Z(\mathrm{j}\omega) = Z^*(-\mathrm{j}\omega)$. If one chooses $y(t) = \mathcal{H}\{x(t)\}$, then single-sidedness is imposed in frequency, $Z(\mathrm{j}\omega) = 0$ for $\omega < 0$, which may also be considered a symmetry in frequency, as we will show. We note that both of these choices may artificially impose symmetry.

In the context of this work, determining the IA/IF of a signal becomes that of determining $y(t)$ and hence $z(t)$ from the observation (or measurement) of $x(t)$, in the most general way possible *without imposing unnecessary constraints*. In the frequency domain, this problem can alternatively be stated as that of determining the *latent spectrum*, $Z(\mathrm{j}\omega) = X(\mathrm{j}\omega) + \mathrm{j}Y(\mathrm{j}\omega)$ from $X(\mathrm{j}\omega)$ where both $X(\mathrm{j}\omega)$ and $Y(\mathrm{j}\omega)$ are complex-valued.

A. The Error in Using the Analytic Signal

As discussed in Section II, the AS is almost universally viewed as the correct way to define a complex signal from the real signal part, and subsequently, the correct way to define IA, IF, and phase for real signals [10]. Next, we make clear that $Z(\mathrm{j}\omega) = 0$ for $\omega < 0$ may be considered as an imposed symmetry in frequency.

We quantify the error in choosing the AS as the correct complex signal by first developing the following symmetry

relations. In the frequency domain, $y_{\mathsf{a}}(t) = \mathcal{H}\{x(t)\}$ implies the FT of the imaginary signal part

$$Y_{\mathsf{a}}(\mathrm{j}\omega) = -\mathrm{j}\,\mathrm{sgn}(\omega)X(\mathrm{j}\omega)$$

and it follows that $Z_{\mathsf{a}}(\mathrm{j}\omega) = 2X(\mathrm{j}\omega)\mathrm{u}(\omega)$ where $\mathrm{u}(\omega)$ is the Heaviside unit step function where $\mathrm{u}(0) = \frac{1}{2}$ [3].

We rewrite the spectrum of an AS in terms of the sign function $\mathrm{u}(\omega) = [\mathrm{sgn}(\omega) + 1]/2$ as

$$Z_{\mathsf{a}}(\mathrm{j}\omega) = \big[1 + \mathrm{sgn}(\omega)\big]X(\mathrm{j}\omega)$$

where it can be shown in terms of frequency symmetries

$$\mathrm{Od}\big\{\mathrm{Im}\{Y_{\mathsf{a}}(\mathrm{j}\omega)\}\big\} = -\mathrm{sgn}(\omega)\mathrm{Ev}\big\{\mathrm{Re}\{X(\mathrm{j}\omega)\}\big\} \tag{9}$$

and

$$\mathrm{Ev}\big\{\mathrm{Re}\{Y_{\mathsf{a}}(\mathrm{j}\omega)\}\big\} = \mathrm{sgn}(\omega)\mathrm{Od}\big\{\mathrm{Im}\{X(\mathrm{j}\omega)\}\big\} \tag{10}$$

where $\mathrm{Im}\{\cdot\}$ is the imaginary operator and $\mathrm{Ev}\{\cdot\}$ and $\mathrm{Od}\{\cdot\}$ denote the even and odd operators, respectively. The symmetry imposed by using the AS is apparent in (9) and (10).

Furthermore, with the error energy defined as

$$E = \int_{-\infty}^{\infty} \big|y_{\mathsf{a}}(t) - y(t)\big|^2\,\mathrm{d}t$$

where $y(t)$ is the true imaginary part, Nuttall derived [30] the spectral error relation

$$E \propto \int_{-\infty}^{0} \big|Z(\mathrm{j}\omega)\big|^2\,\mathrm{d}\omega. \tag{11}$$

In the context of LSA, Nuttall's definition may be reinterpreted as the error between the AS $z_{\mathsf{a}}(t)$ and the latent signal $z(t)$,

$$E = \int_{-\infty}^{\infty} \big|z_{\mathsf{a}}(t) - z(t)\big|^2\,\mathrm{d}t.$$

Expanding (11), we note that this error can be rewritten in terms of frequency symmetry relations as

$$E \propto \int_{-\infty}^{0} \Big|\mathrm{Ev}\big\{\mathrm{Re}\{X(\mathrm{j}\omega)\}\big\} - \mathrm{Od}\big\{\mathrm{Im}\{Y(\mathrm{j}\omega)\}\big\} + \mathrm{j}\,\mathrm{Od}\big\{\mathrm{Im}\{X(\mathrm{j}\omega)\}\big\} + \mathrm{j}\,\mathrm{Ev}\big\{\mathrm{Re}\{Y(\mathrm{j}\omega)\}\big\}\Big|^2\,\mathrm{d}\omega. \tag{12}$$

Equation (12) shows that the error in assuming the AS may be completely determined by asymmetries in the even-real and odd-imaginary parts of both $X(\mathrm{j}\omega)$ and $Y(\mathrm{j}\omega)$. In the case that $y(t) = y_{\mathsf{a}}(t)$, the symmetries in (9) and (10) hold and thus (12) gives a zero error. When $y(t) \neq y_{\mathsf{a}}(t)$ the error may be non-negligible.

VII. Instantaneous Spectral Analysis

We use the term instantaneous spectral analysis (ISA) to refer to a very general framework for TFA consisting of three parts: 1) a parameter set, 2) an instantaneous spectrum, and 3) a signal model. Specifically, in the ISA framework: 1) a signal is represented by a set of canonical triplets $\mathscr{S} = \{\mathscr{C}_0, \mathscr{C}_1, \cdots, \mathscr{C}_{K-1}\}$, 2) each component set has a single-valued mapping to an IS $\mathscr{S} \mapsto \mathcal{S}(t,\omega)$, and 3) each IS has a single-valued mapping to a signal $\mathcal{S}(t,\omega) \mapsto z(t)$.

For the signal model we use the complex AM–FM model as parameterized in Section V. Thus using terminology by Flandrin, the complex AM–FM signal model is a formal *model* because the structure of the analyzed signal is incorporated in the parameterization and is also a formal *decomposition* because the construction process is a linear superposition of time-frequency atoms [11]. In fact, we consider the AM–FM component parameterized by $\mathscr{C}$ in (4) as the most general form of a time-frequency atom.

In this section, we present the main contributions including rigorous definition of the IS, properties of the IS, and relationships of the IS to the FT and TFDs. The IS is both *moving and joint* because it consists of a local description in both time and frequency and *evolutionary* because the coefficients are explicitly time-dependent [11]. The IS is also "*causal*" in the sense of Page and Gupta [31], [32], i.e. the value at time t_0 does not require the signal for $t > t_0$. Although the IS may be considered a "*distribution*" in the sense that it describes the energy allocation in time and frequency, it is not a formal TFD [33] because it is not obtained via an integral transform.

A. Definition of the Instantaneous Spectrum

We define the IS in the *time-frequency coordinates* for a signal expressed with set of canonical triplets $\mathscr{S} = \{\mathscr{C}_0, \mathscr{C}_1, \cdots, \mathscr{C}_{K-1}\}$ as

$$\begin{aligned}\mathcal{S}(t,\omega;\mathscr{S}) &\triangleq 2\pi \sum_{k=0}^{K-1} \int_{-\infty}^{\infty} \psi_k\big(\tau;\mathscr{C}_k\big)\,{}^2\delta\big(t-\tau, \omega - \omega_k(\tau)\big)\,\mathrm{d}\tau \\ &= 2\pi \sum_{k=0}^{K-1} \psi_k\big(t;\mathscr{C}_k\big)\,\delta\big(\omega - \omega_k(t)\big)\end{aligned} \tag{13}$$

where $\delta(\cdot)$ and ${}^2\delta(\cdot,\cdot)$ are 1-D and 2-D Dirac deltas and we have used the well-known sifting property $\int_{-\infty}^{\infty} f(\tau)\,\delta(t-\tau)\,\mathrm{d}\tau = f(t)$ and ${}^2\delta(t,\omega) = \delta(t)\delta(\omega)$ [3].

Theorem The IS, $\mathcal{S}(t,\omega;\mathscr{S})$ maps to signal $z(t;\mathscr{S})$ with

$$\frac{1}{2\pi}\int_{-\infty}^{\infty} \mathcal{S}(t,\omega;\mathscr{S})\,\mathrm{d}\omega = z(t;\mathscr{S}). \tag{14}$$

Proof:

$$\begin{aligned}&\frac{1}{2\pi}\int_{-\infty}^{\infty} \mathcal{S}(t,\omega;\mathscr{S})\,\mathrm{d}\omega \\ &\quad= \frac{1}{2\pi}\int_{-\infty}^{\infty}\left[2\pi\sum_{k=0}^{K-1}\psi_k\big(t;\mathscr{C}_k\big)\,\delta\big(\omega-\omega_k(t)\big)\right]\mathrm{d}\omega \\ &\quad= \sum_{k=0}^{K-1}\psi_k\big(t;\mathscr{C}_k\big)\left[\int_{-\infty}^{\infty}\delta\big(\omega-\omega_k(t)\big)\,\mathrm{d}\omega\right] \\ &\quad= \sum_{k=0}^{K-1}\psi_k\big(t;\mathscr{C}_k\big) \\ &\quad= z(t;\mathscr{S}).\end{aligned}$$

■

The IS defined in (13) is a Dirac-type TFR [34] and may be considered as the ideal TFR [35] in the sense that at any given instant, a component is represented by a weighted Dirac delta at the IF and thus, as will be shown in Section VII-D, is *exactly localized*.

Theorem When $a_k(t) = a_k$, $\omega_k(t) = \omega_k$, and the discrete set takes on a continuum, i.e. $K \to \infty$ where $a_k \to a(\omega)$, $\omega_k \to \omega \in (-\infty, \infty)$, and $\phi_k \to \phi(\omega)$, the IS evaluated at $t = 0$ specializes to the spectrum obtained using the FT[2]

$$\lim_{K\to\infty} \mathcal{S}(0,\omega)\Big|_{\substack{a_k(t)=a_k\\ \omega_k(t)=\omega_k}} = Z(\mathrm{j}\omega). \tag{15}$$

Proof: A limiting form of the IS may be expressed as

$$\begin{aligned}
&\lim_{K\to\infty} \mathcal{S}(t,\omega)\Big|_{\substack{a_k(t)=a_k\\ \omega_k(t)=\omega_k}} \\
&\quad = \lim_{K\to\infty} 2\pi \sum_{k=0}^{K-1} a_k \mathrm{e}^{\mathrm{j}[\omega_k t+\phi_k]}\delta(\omega-\omega_k) \\
&\quad = 2\pi \int_{-\infty}^{\infty} a(\omega)\mathrm{e}^{\mathrm{j}[\omega t+\phi(\omega)]}\delta(\omega-\omega)\,\mathrm{d}\omega \\
&\quad = 2\pi a(\omega)\mathrm{e}^{\mathrm{j}[\omega t+\phi(\omega)]}.
\end{aligned} \tag{16}$$

The corresponding form of the complex AM–FM model is

$$\begin{aligned}
z(t) &= \lim_{K\to\infty} \sum_{k=0}^{K-1} a_k(t)\mathrm{e}^{\mathrm{j}[\int_{-\infty}^{t}\omega_k(\tau)\,\mathrm{d}\tau+\phi_k]}\Big|_{\substack{a_k(t)=a_k\\ \omega_k(t)=\omega_k}} \\
&= \int_{-\infty}^{\infty} a(\omega)\mathrm{e}^{\mathrm{j}[\omega t+\phi(\omega)]}\,\mathrm{d}\omega.
\end{aligned} \tag{17}$$

Setting (17) equal to the inverse FT [36] results in

$$z(t) = \frac{1}{2\pi}\int_{-\infty}^{\infty} Z(\mathrm{j}\omega)\mathrm{e}^{\mathrm{j}\omega t}\,\mathrm{d}\omega = \int_{-\infty}^{\infty} a(\omega)\mathrm{e}^{\mathrm{j}[\omega t+\phi(\omega)]}\,\mathrm{d}\omega.$$

From Lerch's theorem [3]

$$\frac{1}{2\pi}Z(\mathrm{j}\omega) + \cancel{\mathcal{N}(\omega)} = a(\omega)\mathrm{e}^{\mathrm{j}\phi(\omega)}$$

where $\mathcal{N}(\cdot)$ is null function which is ignored for practicality. We then have

$$Z(\mathrm{j}\omega)\mathrm{e}^{\mathrm{j}\omega t} = 2\pi a(\omega)\mathrm{e}^{\mathrm{j}\phi(\omega)}\mathrm{e}^{\mathrm{j}\omega t}$$

and comparison with (16) yields

$$Z(\mathrm{j}\omega)\mathrm{e}^{\mathrm{j}\omega t} = \lim_{K\to\infty} \mathcal{S}(t,\omega)\Big|_{\substack{a_k(t)=a_k\\ \omega_k(t)=\omega_k}}. \tag{18}$$

Equation (18) implies that a limiting form of the IS can be obtained by multiplying $Z(\mathrm{j}\omega)$ with $\mathrm{e}^{\mathrm{j}\omega t}$. Furthermore, while Carson's definition of IF generalizes the notion of frequency, (18) shows that the IS generalizes the notion of a frequency spectrum. Finally, evaluating (18) at $t = 0$ yields

$$Z(\mathrm{j}\omega) = \lim_{K\to\infty} \mathcal{S}(0,\omega)\Big|_{\substack{a_k(t)=a_k\\ \omega_k(t)=\omega_k}}.$$

■

One consideration with the IS is that in general, it is not unique for a particular signal under analysis. That is, in general, there are an infinite number of different sets of canonical triplets $\mathscr{S} = \{\mathscr{C}_0, \mathscr{C}_1, \cdots, \mathscr{C}_{K-1}\}$ and subsequently an infinite number of instantaneous spectra that can be associated with a given complex signal. Despite this non-uniqueness, this framework is advantageous because the inherent ambiguities allow for flexibility in the model. Furthermore, with the proper constraints placed on the model, a unique IS will arise.

[2]Unlike many TFA books, we use the non-unitary, angular frequency FT, and normalization of signal energy is unnecessary.

B. Visualization of the Instantaneous Spectrum

For purposes of interpretation and visualization, we extend (13) by defining a 3-D IS in the *time-frequency-real coordinates* as

$$\mathcal{S}(t,\omega,s;\mathscr{S}) = 2\pi \sum_{k=0}^{K-1} \psi_k\big(t;\mathscr{C}_k\big)\,{}^2\delta\big(\omega-\omega_k(t), s-s_k(t)\big)$$

where $s_k(t)$ is the real part of the kth component, as shown in (6c), and it is understood that the sifting property has been used to rewrite the 3-D Dirac delta as a 2-D Dirac delta similar to (13). We consider the time-frequency-real space as the most intuitive space for interpretation. Integrating out the real dimension, it can be shown that

$$\int_{-\infty}^{\infty} \mathcal{S}(t,\omega,s;\mathscr{S})\,\mathrm{d}s = \mathcal{S}(t,\omega;\mathscr{S}).$$

We can visualize $\mathcal{S}(t,\omega,s)$ by plotting $\omega_k(t)$ vs. $s_k(t)$ vs. t as a line in a 3-D space and coloring the line with respect to $|a_k(t)|$ for each component. Thus, the simultaneous visualization of multiple parameters for each component in the *time-frequency-real* space is possible. Further, orthographic projections of $\mathcal{S}(t,\omega,s)$ yield common plots: the *time-real plane* (the real component waveforms), the *time-frequency plane* (the IS), and the *frequency-real plane* (analogous to the Fourier magnitude spectrum). We consider the 3-D visualization as a type of phase space plot as illustrated in Fig. 3.

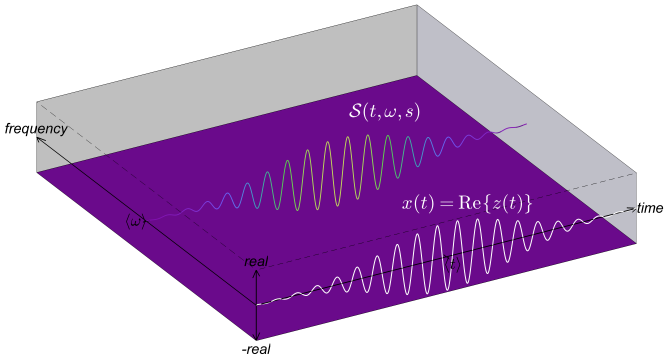

Figure 3. The 3-D instantaneous spectrum $\mathcal{S}(t,\omega,s)$ (—) for a signal consisting of a single Gabor atom $z(t) = a_0\mathrm{e}^{-\pi(t-\langle t\rangle)^2/(2\sigma_t^2)}\mathrm{e}^{\mathrm{j}\langle\omega\rangle(t-\langle t\rangle)}$ with real part shown along the time axis (—).

The complex AM–FM model is motivated by the geometry of complex-valued signals and the interpretation of AM–FM components as rotating vectors in the complex plane as in Fig. 2. For TFA, a complementary interpretation can be developed by considering the 3-D IS as a coordinate system where each component is interpreted as an "illuminated" time-frequency particle or atom, moving in a 3-D space. The reader is referred to the supplementary MPEG-4 file (available at http://ieeexplore.ieee.org) containing an animation illustrating these concepts. The animation illustrates both of these complementary interpretations.

C. Properties of the Instantaneous Spectrum

In Fourier analysis, one studies how transformations of a signal affect the spectrum and vice versa. This is possible

because there is a one-to-one relationship (ignoring null functions) between a signal and the corresponding Fourier spectrum, i.e. $z(t) \overset{\mathcal{F}}{\longleftrightarrow} Z(\mathrm{j}\omega)$. On the other hand, while an IS has a single-valued mapping to a signal, $\mathcal{S}(t,\omega) \mapsto z(t)$, a signal has a multi-valued mapping to an IS, $z(t) \rightrightarrows \mathcal{S}_\kappa(t,\omega),\ \kappa = 1,2,\cdots$. Moreover, while a component set has a single-valued mapping to an IS, $\mathscr{S} \mapsto \mathcal{S}(t,\omega)$, an IS has a multi-valued mapping to a component set, $\mathcal{S}(t,\omega) \rightrightarrows \mathscr{S}_\kappa,\ \kappa = 1,2,\cdots$. Therefore, this implies that we should study how transformations of component sets map to IS transformations and subsequently, map to signal transformations.

There are two basic types of transformations that can be discussed: 1) *component transformations*, i.e. transformations that affect individual components in the set uniquely and 2) *set transformations*, i.e. transformations which affect all signal components in the set uniformly. We consider the latter type and adopt the following notation:

$$\begin{aligned}\mathscr{S}_1 &\mapsto \mathcal{S}_1(t,\omega) \mapsto z_1(t)\\ \mathscr{S}_2 &\mapsto \mathcal{S}_2(t,\omega) \mapsto z_2(t)\\ \mathscr{S} &\mapsto \mathcal{S}(t,\omega) \mapsto z(t).\end{aligned}$$

We will denote a transformation on the set $\mathscr{S}$ of the form $a_k(t) \to f\big(a_k(t)\big)$, $\omega_k(t) \to g\big(\omega_k(t)\big)$, and $\phi_k \to h(\phi_k)$ where $f(\cdot)$, $g(\cdot)$, and $h(\cdot)$ are three functions as

$$\mathscr{S}\Big(f\big(a_k(t)\big),\, g\big(\omega_k(t)\big),\, h(\phi_k)\Big).$$

The following properties then hold.

1) Union (Addition)

$$\mathscr{S}_1 \uplus \mathscr{S}_2 \mapsto \mathcal{S}_1(t,\omega) + \mathcal{S}_2(t,\omega) \mapsto z_1(t) + z_2(t)$$

2) IA Scale and Phase Shift

$$\mathscr{S}(\alpha a_k(t), \omega_k(t), \phi_k + \beta) \mapsto \alpha \mathrm{e}^{\mathrm{j}\beta}\mathcal{S}(t,\omega) \mapsto \alpha \mathrm{e}^{\mathrm{j}\beta} z(t)$$

3) (Real) IA Modulation

$$\mathscr{S}(r(t)a_k(t), \omega_k(t), \phi_k) \mapsto r(t)\mathcal{S}(t,\omega) \mapsto r(t)z(t)$$

4) IF Shift

$$\mathscr{S}(a_k(t), \omega_k(t) + \omega_\mathrm{s}, \phi_k) \mapsto \mathrm{e}^{\mathrm{j}\omega_\mathrm{s} t}\mathcal{S}(t, \omega - \omega_\mathrm{s}) \mapsto \mathrm{e}^{\mathrm{j}\omega_\mathrm{s} t} z(t)$$

5) IA/IF Time-Shift and Re-Reference of Phase

$$\begin{aligned}&\mathscr{S}\Big(a_k(t-t_0), \omega_k(t-t_0), \phi_k - \textstyle\int_{-t_0}^{0} \omega_k(\tau)\,\mathrm{d}\tau\Big)\\ &\quad\mapsto\ \mathcal{S}(t-t_0,\omega) \mapsto z(t-t_0)\end{aligned}$$

6) Phase Function Negation (Conjugation)

$$\mathscr{S}(a_k(t), -\omega_k(t), -\phi_k) \mapsto \mathcal{S}^*(t,-\omega) \mapsto z^*(t)$$

7) Time Reversal and Frequency Negation

$$\mathscr{S}(a_k(-t), -\omega_k(-t), \phi_k) \mapsto \mathcal{S}(-t,-\omega) \mapsto z(-t)$$

8) Similarity (Time and Frequency Scaling)

$$\mathscr{S}(a_k(\alpha t), \alpha\omega_k(\alpha t), \phi_k) \mapsto \frac{1}{|\alpha|}\mathcal{S}\Big(\alpha t, \frac{\omega}{\alpha}\Big) \mapsto z(\alpha t)$$

9) Energy Conservation

$$\frac{1}{2\pi}\int_{-\infty}^{\infty}\left|\int_{-\infty}^{\infty}\mathcal{S}(t,\omega)\,\mathrm{d}\omega\right|^2 \mathrm{d}t = \int_{-\infty}^{\infty}\big|z(t)\big|^2\,\mathrm{d}t$$

D. Relation to Joint Time-Frequency Distributions

In the works by Gabor [7] and Ville [8], they sought a function that describes the energy of the signal simultaneously in time and frequency, where mathematical manipulation may be performed in the same way as with densities [10]. However, the casting of the proposed IS is fundamentally different than these methods. With the exception of the Dirac delta, the IS does not rely on distribution or statistical theory. In particular, there is no use of means, variances, or moments nor joint, conditional, or marginal densities as illustrated in Fig. 4(a). The relation of the IS to TFDs, will now be made formal.

1) Moments of Time and Frequency and Localization: In Gabor's approach [7] the (global) time duration is given by

$$\sigma_t^2 = \int_{-\infty}^{\infty}\big(t - \langle t\rangle\big)^2\big|z(t)\big|^2\,\mathrm{d}t \tag{19}$$

and the (global) bandwidth by

$$\sigma_\omega^2 = \int_{-\infty}^{\infty}\big(\omega - \langle\omega\rangle\big)^2\big|Z(\mathrm{j}\omega)\big|^2\,\mathrm{d}\omega \tag{20}$$

where $\langle t\rangle = \int_{-\infty}^{\infty} t|z(t)|^2\,\mathrm{d}t$ is the (global) mean time and $\langle\omega\rangle = \int_{-\infty}^{\infty}\omega|Z(\mathrm{j}\omega)|^2\,\mathrm{d}\omega$ is the (global) mean frequency. A signal consisting of a single Gaussian AM component, i.e. a Gabor atom $z(t) = a_0\mathrm{e}^{-\pi(t-\langle t\rangle)^2/(2\sigma_t^2)}\mathrm{e}^{\mathrm{j}\langle\omega\rangle(t-\langle t\rangle)}$, minimizes the duration-bandwidth product ${\sigma_t}^2{\sigma_\omega}^2$. Thus, Gabor [7] proposed a discrete TFD given by $P[n,\upsilon] = a_{n,\upsilon}\,\mathrm{e}^{\mathrm{j}\phi_{n,\upsilon}}$ where a signal $z(t)$ is represented as a superposition of Gaussian AM components on a time-frequency lattice

$$z(t) = \sum_{n=-\infty}^{\infty}\sum_{\upsilon=-\infty}^{\infty} a_{n,\upsilon}\,\mathrm{e}^{-\pi(t-n\sigma_t)^2/(2\sigma_t^2)}\mathrm{e}^{\mathrm{j}(\upsilon\sigma_\omega t + \phi_{n,\upsilon})}. \tag{21}$$

Then the limiting form of (21) as $\sigma_t^2 \to 0$ corresponds to time domain analysis and as $\sigma_\omega^2 \to 0$ corresponds to frequency domain analysis. While Gabor's approach has generalized constant amplitude to a Gaussian IA, constant frequency is not generalized to IF, unlike the AM–FM model in (5) which generalizes IA and IF. Both (5) and (21) utilize non-orthogonal components, hence neither can yield a unique representation.

While the Gabor atom is the most localized component when using the duration-bandwidth product as the measure of localization, *this measure depends only on the instantaneous power and the Fourier spectrum of the signal—not on a more general notion of signal localization* [12]. Towards a more general notion, the *global* concepts from Fourier analysis of mean and variance in time and frequency as defined in (19) and (20), may be generalized to *local* concepts of a continuous TFD $P(t,\omega)$ as follows [12]. The variance in frequency at time t or *instantaneous bandwidth* is

$$\sigma_{\omega|t}^2 = \int_{-\infty}^{\infty}\big(\omega - \langle\omega\rangle_t\big)^2 P(\omega\,|\,t)\,\mathrm{d}\omega \tag{22}$$

and the mean frequency at time t is

$$\langle\omega\rangle_t = \int_{-\infty}^{\infty}\omega P(\omega\,|\,t)\,\mathrm{d}\omega \tag{23}$$

where the (conditional) instantaneous density is

$$P(\omega\,|\,t) = \frac{P(t,\omega)}{P(t)} \tag{24}$$

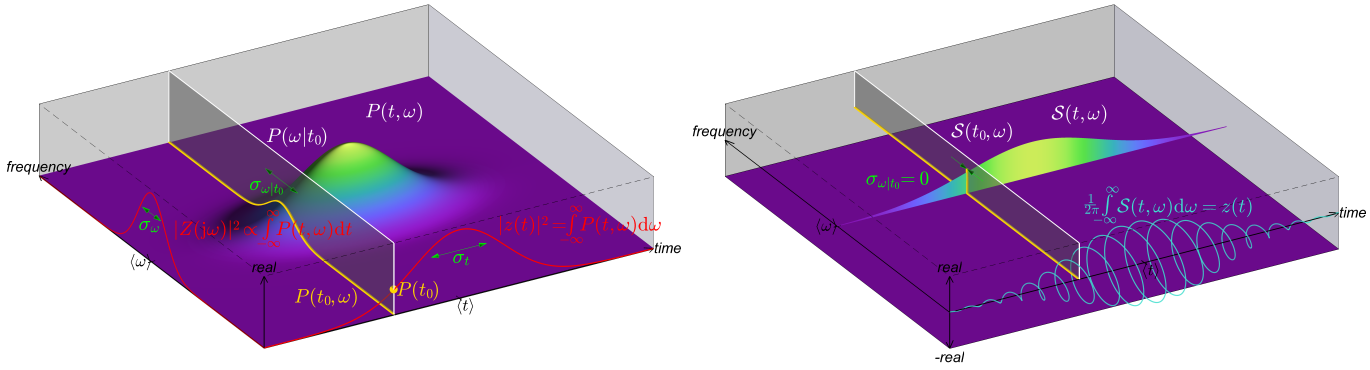

(a) (b)

Figure 4. (a) Illustration of a (positive) time-frequency distribution $P(t,\omega)$ ( ) for a Gabor atom $z(t) = a_0 \mathrm{e}^{-\pi(t-\langle t\rangle)^2/(2\sigma_t^2)} \mathrm{e}^{\mathrm{j}\langle\omega\rangle(t-\langle t\rangle)}$ with instantaneous power $|z(t)|^2$ ( ) and energy spectrum $|Z(\mathrm{j}\omega)|^2$ ( ) shown along the time and frequency axes, respectively. The (conditional) instantaneous density $P(\omega|t) = P(t,\omega)/P(t)$ is highlighted ( ) in the frame ( ) at time t_0. The global descriptors of time duration σ_t^2 ( ) and bandwidth σ_ω^2 ( ) are shown centered at the mean time $\langle t\rangle$ and mean frequency $\langle\omega\rangle$, respectively. The local descriptor, instantaneous bandwidth $\sigma_{\omega|t}^2$ ( ) is shown at t_0 centered about the mean frequency at time t_0, $\langle\omega\rangle_{t_0}$. Note that in the TFD framework, no signal component may have better localization than that of the Gabor atom in the (global) duration-bandwidth sense and furthermore, the instantaneous bandwidth is non-zero. (b) Illustration of interpreting $\mathcal{S}(t,\omega)$ ( ) as a TFD for a Gabor atom $z(t)$ ( ) which is shown along the time axis (imaginary and frequency dimensions overloaded). The instantaneous spectrum at t_0, $\mathcal{S}(t_0,\omega)$ is highlighted ( ) in the frame ( ) at time t_0. The energy is centered in time and frequency at the mean time $\langle t\rangle$ and mean frequency $\langle\omega\rangle$, respectively. The local descriptor, instantaneous bandwidth $\sigma_{\omega|t}^2$ ( ) is shown at t_0 centered about the mean frequency at time t_0, $\langle\omega\rangle_{t_0}$. Note the instantaneous bandwidth $\sigma_{\omega|t}^2 = 0$, thus illustrating that the IS exactly localizes the signal component in an instantaneous bandwidth sense. We note that full-size images of all figures are included as supplemental material available at http://ieeexplore.ieee.org, in order to allow the reader to more carefully examine the fine details.

where $P(t) = \int_{-\infty}^{\infty} P(t,\omega)\,\mathrm{d}\omega$ is the marginal density. Although, some authors generalize localization via the *local* duration-bandwidth product, $\sigma_{\omega|t}^2\sigma_{t|\omega}^2$ [12], we argue that *the more appropriate measure is simply* $\sigma_{\omega|t}^2$ *because this value captures the variance in frequency at an instant in time*. In fact, Cohen in [37] also states that $\sigma_{\omega|t}^2$ is an appropriate localization measure. However, when working with Gabor's framework, only components with constant IA can have zero instantaneous bandwidth [10], [37]—which is not true for the proposed IS.

Theorem The instantaneous spectrum of a monocomponent signal ($K = 1$) exactly localizes the component in frequency at any time instant, i.e. the instantaneous bandwidth $\sigma_{\omega|t}^2 = 0\ \forall\, t$.

Proof: Let $K = 1$ and choose the TFD as

$$P(t,\omega) = \big|\mathcal{S}(t,\omega)\big|.$$

Then using (24) and (23), results in the mean frequency at time t equal to the IF of the component and hence the IF of the signal, i.e. $\langle\omega\rangle_t = \omega_0(t)$. Substituting this result into (22) results in $\sigma_{\omega|t}^2 = 0$ [even when $a_0(t) \neq a_0$]. ■

We note that while the duration-bandwidth product ${\sigma_t}^2{\sigma_\omega}^2$ is lower bounded, for both the instantaneous bandwidth $\sigma_{\omega|t}^2$ and the local duration-bandwidth product $\sigma_{\omega|t}^2\sigma_{t|\omega}^2$ there exists no positive lower bound [12]. Thus, exact localization is possible in the sense that $\sigma_{\omega|t}^2 = 0$ or $\sigma_{\omega|t}^2\sigma_{t|\omega}^2 = 0$, even if ${\sigma_t}^2{\sigma_\omega}^2 \neq 0$. In other words, while the duration-bandwidth may be an appropriate measure of concentration or localization in Fourier analysis, it is simply not an appropriate measure of localization for TFA. These concepts are illustrated in Fig. 4.

2) Time and Frequency Marginals: An alternative approach that builds on Gabor's foundations was suggested by Ville [8], who sought a function $P(t,\omega)$ via an integral transform so that the time marginal yields the instantaneous power

$$\int_{-\infty}^{\infty} P(t,\omega)\,\mathrm{d}\omega = \big|z(t)\big|^2 \tag{25}$$

and frequency marginal yields the energy density spectrum

$$\int_{-\infty}^{\infty} P(t,\omega)\,\mathrm{d}t \propto \big|Z(\mathrm{j}\omega)\big|^2. \tag{26}$$

One distribution that satisfies (25) and (26), is the Wigner-Ville distribution (WVD) [8]

$$\mathrm{WVD}(\tau,\omega) = \int_{-\infty}^{\infty} z\left(\tau+\frac{t}{2}\right) z^*\left(\tau-\frac{t}{2}\right)\mathrm{e}^{-\mathrm{j}\omega t}\,\mathrm{d}t$$

where τ is a time variable. For a monocomponent signal consisting of a complex linear chirp, the WVD results in a weighted Dirac delta at the IF. Thus, in Ville's approach the complex linear chirp is *exactly localized in frequency in the sense that the instantaneous bandwidth* $\sigma_{\omega|t}^2 = 0$, however, for other signals including other monocomponent signals, this is generally not true [8]–[12], [14], [35].

On the contrary, rather than seeking $P(t,\omega)$ to satisfy (25) and (26), the proposed IS, by definition, results in somewhat analogous relationships given in (14) and (15). First, (14) is a stronger form of (25) because $z(t)$ may be recovered exactly. Second, (26) forces alignment with the Fourier spectrum whereas the IS specializes to the Fourier spectrum via (15).

3) Time-Frequency Distributions: TFDs are generally classified by which properties they satisfy. Cohen's quadratic class are the quadratic TFDs which satisfy the marginals and preserve time-shifts and frequency-shifts [33]

$$\mathrm{C}_{\mathfrak{k}}(\tau,\omega) = \int_{-\infty}^{\infty}\int_{-\infty}^{\infty}\int_{-\infty}^{\infty} z\left(\tau+\frac{t}{2}\right) z^*\left(\tau-\frac{t}{2}\right) \times \mathfrak{k}(t,\omega)\mathrm{e}^{\mathrm{j}(\omega\tau-\omega\tau-\omega t)}\,\mathrm{d}\omega\,\mathrm{d}\tau\,\mathrm{d}t$$

with free parameter $\mathfrak{k}(t,\omega)$ the *kernel* function [9]. Choosing $\mathfrak{k}(t,\omega) = 1$ yields the WVD and choosing $\mathfrak{k}(t,\omega) = \exp[-\gamma(t\omega)^2]$ yields the Choi-Williams distribution (CWD) with parameter $\gamma \geq 0$ [38]; as $\gamma \to 0$, the CWD is the WVD. Similarly, the affine class are the quadratic TFDs which satisfy the marginals and preserve time-shifts and frequency-scales. Another special class of TFDs are the linear TFDs, which include the short-time Fourier transform (STFT) [39]

$$\mathrm{STFT}_w(\tau,\omega) = \int_{-\infty}^{\infty} z(t) w(t-\tau) \mathrm{e}^{-\mathrm{j}\omega t}\,\mathrm{d}t$$

with free-parameter $w(t)$ the *window* function and the wavelet transform (WT) [40]

$$\mathrm{WT}_w(\tau,c) = \int_{-\infty}^{\infty} z(t) \sqrt{|c|}\, w^*\!\left(\frac{t-\tau}{c}\right) \mathrm{d}t$$

with free-parameter $w(t)$ the mother *wavelet*. The WT is unique among TFDs because it has the linearity, time-shift, and frequency-scale properties [9]–[12]. However, the independent variable c is not strictly a frequency variable but rather a scale variable and thus will not be considered in the examples in Section VIII. The spectrogram and scalogram are the quadratic TFDs defined as the magnitude-squared of the STFT, $\mathrm{SPEC}_w(\tau,\omega) = |\mathrm{STFT}_w(\tau,\omega)|^2$ and WT, $\mathrm{SCAL}_w(\tau,\omega) = |\mathrm{WT}_w(\tau,c)|^2$. Finally, the STFT is unique among TFDs because it has the linearity, time-shift, and frequency-shift properties. Therefore, the fact that the IS satisfies linearity (addition, IA scale, and phase shift) as well as preserves time-shifts and frequency-shifts, but is not in general equivalent to the STFT, implies that the IS is not a traditional *time-frequency distribution* but is a more general type of *time-frequency representation*.

VIII. Examples

In this section, we demonstrate use of the IS for three classic examples drawn from the time-frequency literature [10]. These examples show for particular parameter sets the corresponding instantaneous spectra and give expressions for the associated signals. Finally, the IS is shown to have distinct conceptual advantages by way of interpretation when compared against some of the most common TFDs including the STFT, WVD, and CWD.

A. Sinusoidal AM Example

Suppose we have a component set $\mathscr{S}_1$ consisting of a single component

$$\mathscr{C}_0 = \left(2\cos\!\left(\frac{1}{2}(\omega_\mathrm{b}-\omega_\mathrm{a})t\right),\quad \frac{(\omega_\mathrm{b}+\omega_\mathrm{a})}{2},\quad 0\right)$$

where ω_a and ω_b are constants. The corresponding IS, $\mathscr{S}_1 \mapsto \mathcal{S}_1(t,\omega)$ is illustrated in Fig. 5(a). Suppose we have another component set $\mathscr{S}_2$ consisting of two components

$$\mathscr{C}_0 = \big(1,\ \omega_\mathrm{a},\ 0\big) \quad \text{and} \quad \mathscr{C}_1 = \big(1,\ \omega_\mathrm{b},\ 0\big).$$

The corresponding IS, $\mathscr{S}_2 \mapsto \mathcal{S}_2(t,\omega)$ is illustrated in Fig. 5(b) and it may be clearly seen that $\mathcal{S}_1(t,\omega) \neq \mathcal{S}_2(t,\omega)$. Subsequently, $\mathcal{S}_1(t,\omega) \mapsto z_1(t)$ and $\mathcal{S}_2(t,\omega) \mapsto z_2(t)$ where

$$z_1(t) = 2\cos\!\left(\frac{1}{2}(\omega_\mathrm{b}-\omega_\mathrm{a})t\right)\mathrm{e}^{\mathrm{j}\left[\frac{1}{2}(\omega_\mathrm{b}+\omega_\mathrm{a})t\right]} \tag{27a}$$

$$z_2(t) = \mathrm{e}^{\mathrm{j}\omega_\mathrm{a}t} + \mathrm{e}^{\mathrm{j}\omega_\mathrm{b}t} \tag{27b}$$

are the same sinusoidal AM signal, i.e. $z_1(t) = z_2(t)$. While mathematically there is no difference between (27a) and (27b) other than how the signal has been expressed, there may be reasons to prefer a particular spectrum, $\mathcal{S}_1(t,\omega)$ or $\mathcal{S}_2(t,\omega)$. For example, assuming the signal is latent $z_1(t) = z_2(t) \mapsto x(t)$, the human auditory system perceives $x(t)$ as a single AM tone (corresponding to $\mathscr{S}_1$) if ω_a and ω_b are not sufficiently far apart and perceives two distinct constant tones (corresponding to $\mathscr{S}_2$) if ω_a and ω_b are sufficiently far apart [41]. Thus, these two perceptions can each be associated with a particular IS, $\mathcal{S}_1(t,\omega)$ or $\mathcal{S}_2(t,\omega)$, even though the signals are mathematically identical. For comparison, several TFDs for the sinusoidal AM signal in (27) are provided in Figs. 5(c)-(f), with commentary provided in the caption.

B. Sinusoidal FM Example

Suppose we have a component set $\mathscr{S}_1$ consisting of a single component

$$\mathscr{C}_0 = \left(1,\quad \omega_0 - B\sin(\omega_\mathrm{m}t),\quad \frac{B}{\omega_\mathrm{m}}\right)$$

where ω_0, ω_m, and B are constants. The corresponding IS, $\mathscr{S}_1 \mapsto \mathcal{S}_1(t,\omega)$ is illustrated in Fig. 6(a). Suppose we have another component set $\mathscr{S}_2$ consisting of an infinite number of components where $\mathscr{S}_2 = \{\mathscr{C}_k\}$ with $k = 0, 1, \cdots$ and

$$\mathscr{C}_k = \Big(\mathrm{J}_\ell\big(2\pi B/\omega_\mathrm{m}\big),\ \omega_0 + \ell\omega_\mathrm{m},\ \ell\frac{\pi}{2}\Big)$$

where $\ell = k/2$ for even k, $\ell = -(k+1)/2$ for odd k, and $\mathrm{J}_\ell(\cdot)$ denotes the ℓth-order Bessel function of the first kind [1]. The corresponding IS, $\mathscr{S}_2 \mapsto \mathcal{S}_2(t,\omega)$ is illustrated in Fig. 6(b) and it may be clearly seen that $\mathcal{S}_1(t,\omega) \neq \mathcal{S}_2(t,\omega)$. Subsequently, $\mathcal{S}_1(t,\omega) \mapsto z_1(t)$ and $\mathcal{S}_2(t,\omega) \mapsto z_2(t)$ where

$$z_1(t) = \mathrm{e}^{\mathrm{j}\left[\omega_0 t + \frac{B}{\omega_\mathrm{m}}\cos(\omega_\mathrm{m}t)\right]} \tag{28a}$$

$$z_2(t) = \sum_{\ell=-\infty}^{\infty} \mathrm{J}_\ell(2\pi B/\omega_\mathrm{m})\mathrm{e}^{\mathrm{j}[(\omega_0+\ell\omega_\mathrm{m})t+\ell\frac{\pi}{2})]} \tag{28b}$$

are the same sinusoidal FM signal, i.e. $z_1(t) = z_2(t)$. Again, while mathematically there is no difference between (28a) and (28b) other than how the signal has been expressed, there may be reason to prefer a particular spectrum, $\mathcal{S}_1(t,\omega)$ or $\mathcal{S}_2(t,\omega)$. For example, assuming the signal is latent $z_1(t) = z_2(t) \mapsto x(t)$, the human auditory system may perceive $x(t)$ as a single FM tone (corresponding to $\mathscr{S}_1$) [4]. Thus, $\mathcal{S}_1(t,\omega)$ can align with perception even though $\mathcal{S}_2(t,\omega)$ is also a valid IS that can be associated with the same signal. For comparison, several TFDs for the sinusoidal FM signal in (28) are provided in Figs. 6(c)-(f), with commentary provided in the caption.

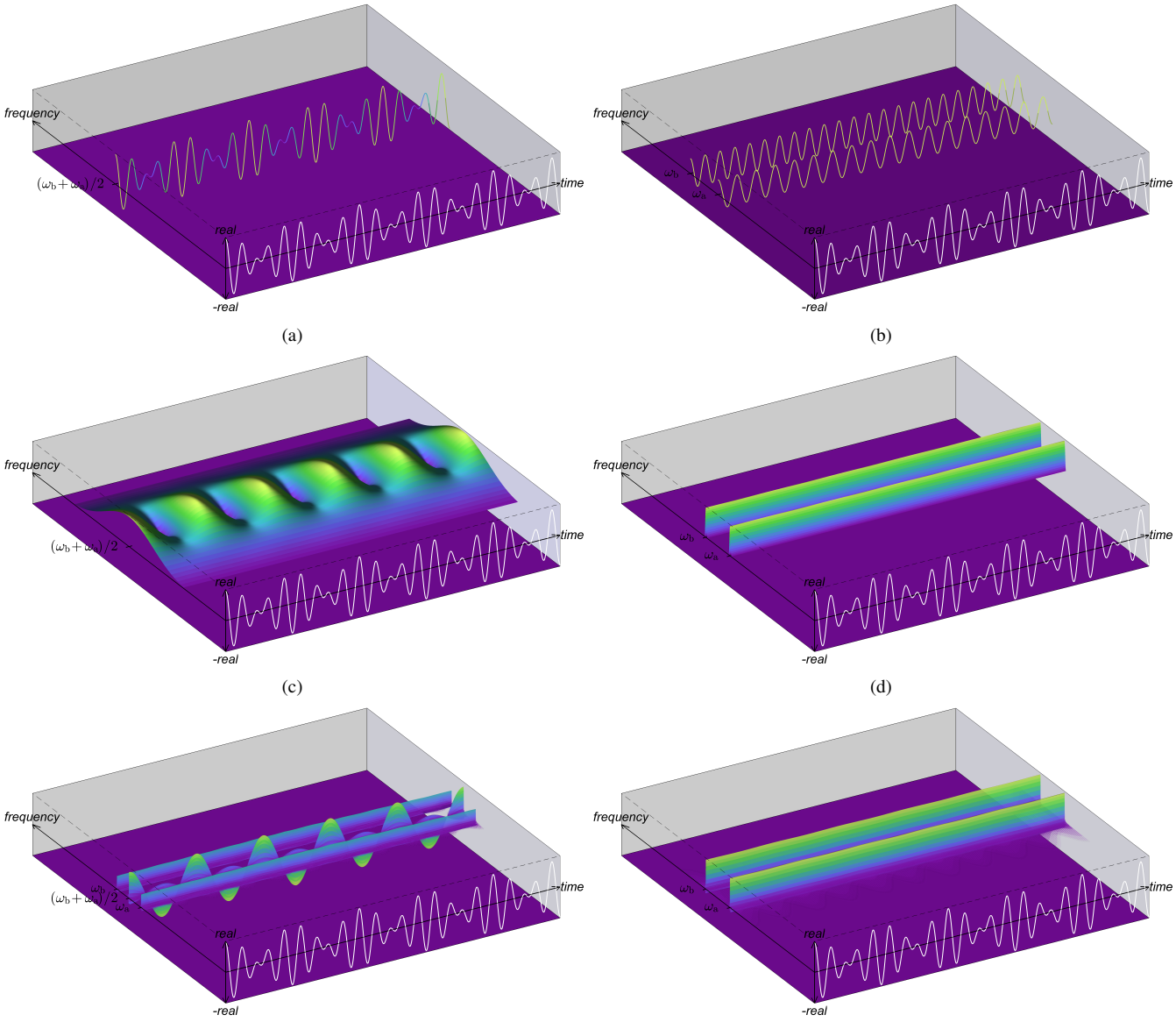

Figure 5. For the sinusoidal AM signal in (27) the (a) IS with a single AM component, (b) IS with two components each having constant IA and constant IF, (c) STFT magnitude with a relatively short Hamming window (wideband STFT), (d) STFT magnitude with a relatively long Hamming window (narrowband STFT), (e) Wigner-Ville distribution, and (f) Choi-Williams distribution with parameter $\gamma = 1$. For all plots the corresponding real signal is shown along the time axis. The wideband STFT in (c) shows general energy alignment with $\mathcal{S}_1(t,\omega)$ in (a), i.e. the energy oscillations in amplitude are in sync with one another and the peak values align in time and frequency. However unlike $\mathcal{S}_1(t,\omega)$, the instantaneous bandwidth of the STFT is not zero. While increasing the window length decreases the instantaneous bandwidth, the end result is a STFT that aligns with (b) not (a). Similarly, we see that the narrowband STFT in (d) has a general energy alignment with $\mathcal{S}_2(t,\omega)$ in (b), i.e. the energy is constant near frequencies ω_a and ω_b. Although the instantaneous bandwidth about each component of the STFT is not zero, unlike in $\mathcal{S}_2(t,\omega)$, it may be made arbitrarily small by increasing the window length. The WVD is shown in (e), where we see oscillating energy at $\frac{\omega_\mathrm{b}+\omega_\mathrm{a}}{2}$ as in $\mathcal{S}_1(t,\omega)$ and constant energy at ω_a and ω_b as in $\mathcal{S}_2(t,\omega)$. In this example, instantaneous bandwidth about each of the three frequencies is zero. In between the oscillatory peaks, the WVD takes on negative values that align with low IA values of the component in $\mathscr{S}_1$ and furthermore, the negative peaks in the WVD align with sign changes of the IA of the IS shown in (a). The occurrence of negative values in the WVD is well-established and prevents straightforward and intuitive interpretation. In the CWD shown in (f), as γ increases from zero the energy in the oscillatory term in (e) is suppressed at the expense of increased instantaneous bandwidth [38] about the two remaining constant energy terms. Unlike the IS and WVD, the STFTs and CWD are unable to achieve zero instantaneous bandwidth about the signal components. However, unlike the IS which allows two representations each with distinct interpretation, the WVD provides only a single representation that may not allow for intuitive interpretation. We note that full-size images of all figures are included as supplemental material available at http://ieeexplore.ieee.org, in order to allow the reader to more carefully examine the fine details. All WVDs and CWDs in this paper were computed using the TFSAP toolbox [9].

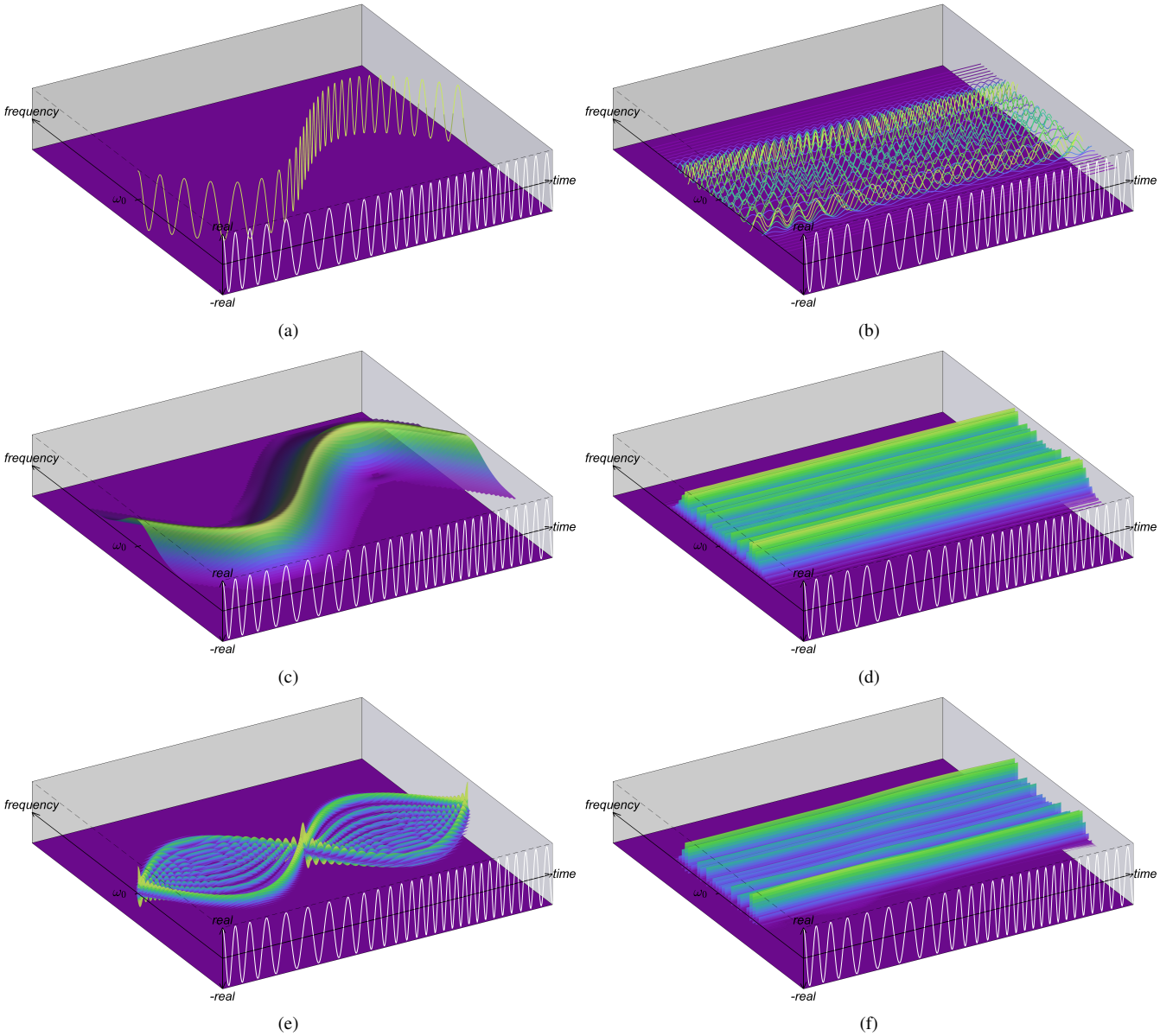

Figure 6. For the sinusoidal FM signal in (28) the (a) IS with a single FM component, (b) IS with an infinite number of components each having constant IA and constant IF, (c) STFT magnitude with a relatively short Hamming window (wideband STFT), (d) STFT magnitude with a relatively long Hamming window (narrowband STFT), (e) Wigner-Ville distribution, and (f) Choi-Williams distribution with parameter $\gamma = 1$. For all plots the corresponding real signal is shown along the time axis. The wideband STFT in (c) shows general energy alignment with $\mathcal{S}_1(t,\omega)$ in (a), i.e. the energy oscillations in frequency are aligned with one another and the peak values align in time and frequency. However unlike $\mathcal{S}_1(t,\omega)$, the instantaneous bandwidth of the STFT is not zero. While increasing the window length decreases the instantaneous bandwidth, the end result is an STFT that aligns with (b) not (a). Similarly, we see that the narrowband STFT in (d) has a general energy alignment with $\mathcal{S}_2(t,\omega)$ in (b), i.e. the energy is constant at harmonic frequencies. Although the instantaneous bandwidth about each component of the STFT is not zero, unlike in $\mathcal{S}_2(t,\omega)$, it may be made arbitrarily small by increasing the window length. The WVD is shown in (e) and although there is some energy alignment with (a), the presence of significant cross-terms prevents intuitive interpretation. The CWD shown in (f) shows general energy alignment with $\mathcal{S}_2(t,\omega)$. Unlike the IS, the STFTs, WVD, and CWD are unable to achieve zero instantaneous bandwidth about the signal components. We note that full-size images of all figures are included as supplemental material available at http://ieeexplore.ieee.org, in order to allow the reader to more carefully examine the fine details. All WVDs and CWDs in this paper were computed using the TFSAP toolbox [9].

C. Gaussian AM Chirp, FM Chirp Example

Suppose we have a component set $\mathscr{S}$ consisting of a single component

$$\mathscr{C}_0 = \left(te^{\frac{-\alpha t^2}{2}}, \quad \omega_0 + \beta t, \quad 0\right)$$

where α and β, are constants. The corresponding IS, $\mathscr{S} \mapsto \mathcal{S}(t,\omega)$ is illustrated in Fig. 7(a). Subsequently, $\mathcal{S}(t,\omega) \mapsto z(t)$ where

$$z(t) = te^{\frac{-\alpha t^2}{2}} e^{\mathrm{j}\left[\omega_0 t + \frac{\beta}{2}t^2\right]} \tag{29}$$

is a Gaussian AM chirp, FM chirp signal. For comparison, several TFDs for the signal in (29) are provided in Figs. 7(b)-(d), with commentary provided in the caption.

IX. Discussion

At its heart, the TFA problem is that of signal representation. Traditional TFD analysis provides a mathematical framework which is similar to distribution theory, while ISA provides a mathematical framework which is similar to a coordinate system. Formally, the TFA problem may be stated as follows. When using TFD framework, for a given signal $z(t)$ or $x(t)$ find $P(t,\omega)$ subject to

$$\begin{aligned} z(t) &\mapsto P(t,\omega) \quad \text{or} \\ x(t) &\mapsto P(t,\omega) \quad \text{or} \\ x(t) \overset{\text{Eqn. (1)}}{\longmapsto} z_{\mathsf{a}}(t) &\mapsto P(t,\omega) \end{aligned}$$

via an integral transform acting on the signal. When using IS framework, for a given signal $z(t)$ or $x(t)$ find $\mathscr{S}$ subject to

$$\mathscr{S} \overset{\text{Eqn. (13)}}{\longmapsto} \mathcal{S}(t,\omega) \overset{\text{Eqn. (14)}}{\longmapsto} z(t) \overset{\text{Eqn. (8)}}{\longmapsto} x(t).$$

Regardless of the time-frequency framework chosen for representation, the problem is not, in general, uniquely solvable because the problem is under-constrained—providing few general mathematical constraints and allowing for infinite degrees of freedom. This under-determinedness manifests in TFD analysis as an infinite number of possible TFDs to choose from based on desirable properties and manifests in ISA as an infinite number of ways to decompose a signal into a sum of parts, each leading to a different IS. On one hand, TFD theory has has seen incremental advances in recent years, however as Cohen writes [10], "[t]he current state of affairs is that we do not have a complete theory." On the other hand, ISA has unique and powerful advantages over TFD analysis because the IS is both linear and exactly localizes all signal components in time-frequency. Moreover, the very act of expressing a signal $z(t)$ in the appropriate written form $z(t;\mathscr{S})$ as in (5), has the effect of imposing a structure upon the signal, yielding a parameter set $\mathscr{S}$ which uniquely maps to an IS $\mathcal{S}(t,\omega;\mathscr{S})$.

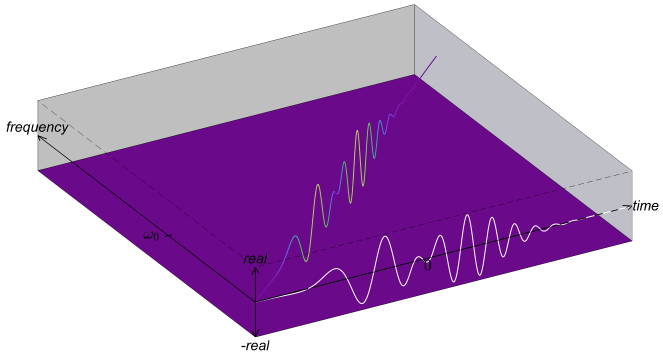

(a)

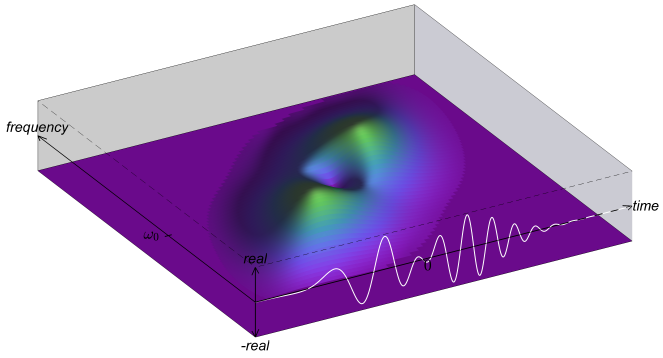

(b)

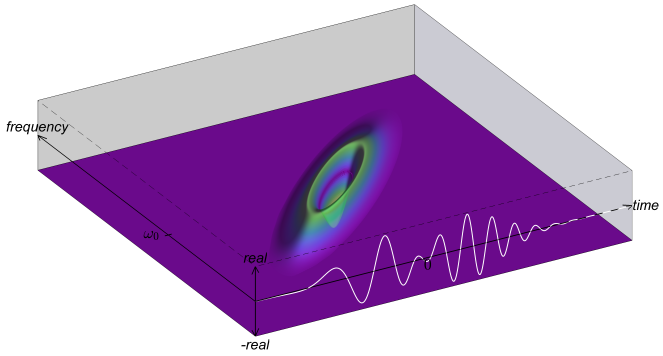

(c)

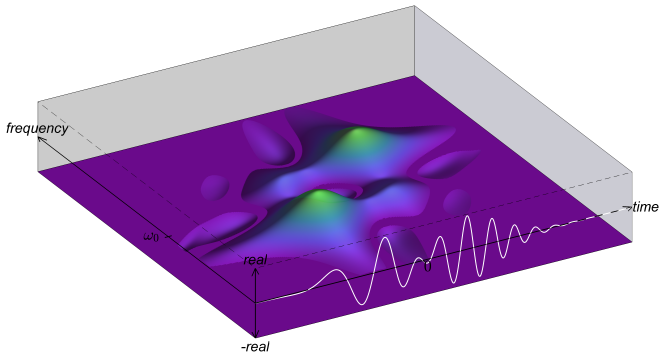

(d)

Figure 7. For the Gaussian AM chirp, FM chirp signal in (29) the (a) IS with a single component, (b) STFT magnitude for a moderate length Hamming window, (c) WVD, and (d) CWD with parameter $\gamma = 1$. For all plots the corresponding real signal is shown along the time axis. The STFT in (b) shows general energy alignment with $\mathcal{S}(t,\omega)$ in (a), i.e. the energy peaks align in time and frequency. However unlike $\mathcal{S}(t,\omega)$, the instantaneous bandwidth of the STFT is not zero. The WVD shown in (c) is negative in the center of the figure, when $\alpha t^2 + (\omega - \beta - \omega_0)^2/\alpha \leq \frac{1}{2}$ [10] and the negative peak aligns with the sign change of the component shown in (a). The CWD shown in (d) shows general energy alignment with $\mathcal{S}(t,\omega)$ in (a), i.e. the energy peaks align in time and frequency.

Finally, it is important to clearly distinguish between the ISA theory proposed in this work, which utilizes a complex AM–FM model, and specific algorithms for computing the parameters of an AM–FM model, i.e. a signal decomposition. While both the proposed theory and these algorithms use the AM–FM model parameters to define a TFR, there is a critical difference which results in important theoretical implications: our definition of the IS in (13) includes the appropriate phase which admits the important properties given in Section VII-C. These properties hold regardless of the specific algorithm used for computing the parameters and of the particular signal under analysis. In fact, any algorithm which produces, either directly or indirectly, a set of AM–FM model parameters is compatible with the proposed theory and can be used to specify an IS possessing the properties we have described. However, we do not advocate any particular decomposition because in general there is no single algorithm that can perform satisfactorily for all signals. Nevertheless, in order for the proposed IS to be useful in practical applications a decomposition algorithm is required. Therefore, a brief review of signal decomposition algorithms [42]–[47] compatible with the proposed IS is provided in Appendix A.

X. Conclusions

In this paper, we developed a generalized mathematical framework for TFA by defining an IS which generalizes the notion of the Fourier spectrum and in which the notion of generalized frequency, i.e. IF is utilized to the fullest extent. Unlike previous attempts to define a generalized spectrum, we believe that ties with the FT and HT, in general, must be severed and maintained only in special cases. This is in contrast to TFDs which require at a minimum one FT and often one HT. While other Dirac-type TFRs based on an AM–FM model are common in the literature, our definition utilizes an appropriately chosen phase term which gives rise to several convenient mathematical properties. We highlighted that the AS may artificially impose frequency symmetries and by giving up the AS, we allowed for alternative complex extensions and hence alternative IA/IF parameterizations for a real signal that may be more useful. We utilized a carefully parameterized signal model based on a superposition of complex AM–FM components which uses Carson's original IF definition, but without the restrictions of the AS. This model allows for a signal parameterization using a set of canonical triplets, which are interpreted as the coordinates in time and frequency and are used to define the IS. Additionally, for interpretation, we proposed a 3-D IS and a corresponding 3-D visualization. We discussed the relationship of the proposed IS to the FT and TFDs, pointing out several important differences.

Appendix A
Computational AM–FM Models

In this appendix we provide a brief review of several algorithms for AM–FM modeling compatible with the proposed IS, noting that additional reviews may also be found in [48]–[50]. Some of the earliest examples of AM–FM models are those based on the HT [51]–[56] and the Teager energy separation algorithm (TESA) [42], [48], [57]–[64]. Both the HT and TESA permit the estimation of IA and IF of any real signal, but do not address signal decomposition. As a result, methods for using the HT and TESA for decomposition have been proposed.

Another category of AM–FM models are based on ridge tracking/sinusoidal modeling [43], [65]–[67]. In ridge tracking, it is assumed that each component appears in a TFD as a single ridge of energy concentration. Thus, a signal can be parameterized by tracking its ridges in location, intensity, and possibly bandwidth. The TFD is usually derived from a STFT [43] but a more general TFD can also be used [65]. Extensions of the sinusoidal model have been proposed, such as the harmonic plus noise and adaptive quasi-harmonic model [66]. Also related to ridge tracking are the empirical wavelet [68] and synchrosqueezed wavelet transforms [29], [47], [69].

More recently mode decomposition algorithms, such as the empirical mode decomposition (EMD) and its variations, have also been used to compute AM–FM parameters [27], [45], [46], [70], [71]. Alternate formulations of EMD, which are more mathematically grounded, have also been proposed including techniques based on optimization [72]–[74], machine learning [75], PDEs [76]–[81], rolling balls [82], [83], iterative filtering [84], [85], and Fourier analysis [86]. Extensions to EMD include the complex EMD and multi-variate EMD [87]–[92] and multi-dimensinal EMD [93]–[97]. Other examples of mode decompositions include, variational (non-linear chirp) mode [44], [98], [99], local mean [100], intrinsic time-scale [98], nonlinear mode [101], local characteristic scale [102], and adaptive local iterative filtering [85] decompositions.

Acknowledgments

The authors wish to thank Prof. Joe Lakey of the Dept. of Mathematical Sciences at New Mexico State University; Prof. Antonia Papandreou-Suppappola of the School of Electrical, Computer and Energy Engineering at Arizona State University; and Prof. Laura Boucheron of the Klipsch School of Electrical and Computer Engineering at New Mexico State University for reviewing early drafts of this manuscript.

References

[1] E. C. Titchmarsh, *Introduction to the Theory of Fourier Integrals*. Clarendon Press Oxford, 1948.
[2] A. Papoulis, *The Fourier Integral and Its Applications*. McGraw-Hill, 1960.
[3] R. Bracewell, *The Fourier Transform and Its Applications*. McGraw-Hill, 1980.
[4] J. R. Carson, "Notes on the theory of modulation," *Proc. IRE*, vol. 10, no. 1, pp. 57–64, Feb. 1922.
[5] J. R. Carson and T. C. Fry, "Variable frequency electric circuit theory," *Bell Syst. Tech. J.*, vol. 16, pp. 513–540, Oct. 1937.
[6] B. V. D. Pol, "The fundamental principles of frequency modulation," *J. Inst. Electr. Eng. 3*, vol. 93, no. 23, pp. 153–158, May 1946.
[7] D. Gabor, "Theory of communication. part 1: the analysis of information," *J. Inst. Electr. Eng. 3*, vol. 93, no. 26, pp. 429–441, Nov. 1946.
[8] J. Ville, "Theorie et applications de la notion de signal analytique," *Cables et Transmission*, vol. 2a, pp. 61–74, 1948.
[9] B. Boashash, Ed., *Time Frequency Signal Analysis and Processing*. Elsevier, 2003.
[10] L. Cohen, *Time-Frequency Analysis*. Prentice Hall, 1995.
[11] P. Flandrin, *Time-Frequency/Time-Scale Analysis*. Academic press, 1998, vol. 10.

[12] A. Papandreou-Suppappola, Ed., *Applications in Time-Frequency Signal Processing*. CRC press, 2002.

[13] N. E. Huang, X. Chen, M. Lo, and Z. Wu, "On Hilbert spectral representation: a true time-frequency representation for nonlinear and nonstationary data," *Adv. Adapt. Data Anal.*, vol. 3, no. 1 & 2, pp. 63–93, 2011.

[14] L. Stanković, M. Daković, and T. Thayaparan, *Time-frequency signal analysis with applications*. Artech house, 2014.

[15] S. G. Krantz, *Explorations in harmonic analysis: with applications to complex function theory and the Heisenberg group*. Springer Science & Business Media, 2009.

[16] C. W. Therrien, "The Lee-Wiener legacy [statistical theory of communication]," *IEEE Signal Process. Mag.*, vol. 19, no. 6, pp. 33–34, Nov. 2002.

[17] A. Papoulis, *Signal Analysis*. McGraw-Hill New York, 1977.

[18] D. E. Vakman, "On the definition of concepts of amplitude phase and instantaneous frequency," *Radio Eng. and Electron. Phys.*, vol. 17, pp. 754–759, 1972.

[19] ——, "Do we know what are the instantaneous frequency and instantaneous amplitude of a signal," *Radio Eng. and Electron. Phys.*, vol. 21, pp. 95–100, 1976.

[20] ——, "Measuring the frequency of an analytical signal," *Radio Eng. and Electron. Phys.*, vol. 24, pp. 63–69, 1979.

[21] L. Cohen, P. Loughlin, and D. Vakman, "On an ambiguity in the definition of the amplitude and phase of a signal," *Signal Process.*, vol. 79, no. 3, pp. 301–307, 1999.

[22] D. Vakman, *Signals, Oscillations and Waves*. Artech House, 1998.

[23] B. Boashash, "Estimating and interpreting the instantaneous frequency of a signal. I: fundamentals," *Proc. IEEE*, vol. 80, no. 4, pp. 520–538, Apr. 1992.

[24] J. Shekel, " 'Instantaneous' frequency," *Proc. IRE*, vol. 41, no. 4, pp. 548–548, Apr. 1953.

[25] L. M. Fink, "Relations between the spectrum and instantaneous frequency of a signal," *Problemy Peredachi Informatsii*, vol. 2, no. 4, pp. 26–38, 1966.

[26] L. Mandel, "Interpretation of instantaneous frequencies," *Am. J. of Phys.*, vol. 42, no. 10, pp. 840–846, 1974.

[27] N. E. Huang, Z. Shen, S. R. Long, M. C. Wu, H. H. Shih, Q. Zheng, N. C. Yen, C. C. Tung, and H. H. Liu, "The empirical mode decomposition and the Hilbert spectrum for nonlinear and non-stationary time series analysis," *Proc. R. Soc. London Ser. A*, vol. 454, no. 1971, pp. 903–995, Mar. 1998.

[28] B. Picinbono, "On instantaneous amplitude and phase of signals," *IEEE Trans. Signal Process.*, vol. 45, no. 3, pp. 552–560, Mar. 1997.

[29] C. K. Chui and H. K. Mhaskar, "Signal decomposition and analysis via extraction of frequencies," *Appl. Comput. Harmonic Anal.*, vol. 40, no. 1, pp. 97–136, 2016.

[30] A. H. Nuttall and E. Bedrosian, "On the quadrature approximation to the Hilbert transform of modulated signals," *Proc. IEEE*, vol. 54, no. 10, pp. 1458–1459, Oct. 1966.

[31] C. Page, "Instantaneous power spectra," *J. Appl. Phys.*, vol. 23, no. 1, pp. 103–106, 1952.

[32] M. S. Gupta, "Definition of instantaneous frequency and frequency measurability," *Am. J. of Phys.*, vol. 43, no. 12, pp. 1087–1088, 1975.

[33] L. Cohen, "Time-frequency distributions–a review," *Proc. IEEE*, vol. 77, no. 7, pp. 941–981, 1989.

[34] L. Zhang, T. Qian, W. Mai, and P. Dang, "Adaptive Fourier decomposition-based Dirac type time-frequency distribution," *Math Methods Appl. Sci.*, 2016.

[35] S. Meignen, T. Oberlin, and H. T. Wu, "Time-frequency reassignment and synchrosqueezing," *IEEE Signal Process. Mag.*, Nov. 2013.

[36] A. V. Oppenheim, A. Willsky, and S. H. Nawab, *Signals and Systems*, 2nd ed. Prentice Hall, 1997.

[37] B. Boashash, Ed., *Time-Frequency Signal Analysis–Methods and Applications*. Longman Publishing Group, 1992.

[38] M. Akay, Ed., *Time Frequency and Wavelets in Biomedical Signal Processing*. IEEE press, 1998.

[39] L. Montgomery and I. Reed, "A generalization of the Gabor-Helstrom transform," *IEEE Trans. Inf. Theory*, vol. 13, no. 2, pp. 344–354, 1967.

[40] S. Mallat, *A Wavelet Tour of Signal Processing*. Academic press, 1999.

[41] D. O'Shaughnessy, *Speech Communication: Human and Machine*. Addison-Wesley Pub. Co., 1987.

[42] A. O. Boudraa, "Instantaneous frequency estimation of FM signals by ψ_b-energy operator," *Electron. Lett.*, vol. 47, no. 10, pp. 623–624, 2011.

[43] R. McAulay and T. F. Quatieri, "Speech analysis/synthesis based on a sinusoidal representation," *IEEE Trans. Acoust., Speech, Signal Process.*, vol. 34, no. 4, pp. 744–754, Aug. 1986.

[44] K. Dragomiretskiy and D. Zosso, "Variational mode decomposition," *IEEE Trans. Signal Process.*, vol. 62, no. 3, pp. 531–544, 2014.

[45] M. E. Torres, M. A. Colominas, G. Schlotthauer, and P. Flandrin, "A complete ensemble empirical mode decomposition with adaptive noise," in *Proc. IEEE Int. Conf. Acoust. Speech Signal Process.*, 2011, pp. 4144–4147.

[46] M. A. Colominas, G. Schlotthauera, and M. E. Torres, "Improved complete ensemble EMD: a suitable tool for biomedical signal processing," *Biomed. Signal. Process. Control*, vol. 14, pp. 19–29, Nov. 2014.

[47] D. I, J. Lu, and H. T. Wu, "Synchrosqueezed wavelet transforms: an empirical mode decomposition-like tool," *Appl. Comput. Harmonic Anal.*, vol. 30, no. 2, pp. 243–261, 2011.

[48] B. Santhanam and P. Maragos, "Multicomponent AM–FM demodulation via periodicity-based algebraic separation and energy-based demodulation," *IEEE Trans. Commun.*, vol. 48, no. 3, pp. 473–490, 2000.

[49] F. Gianfelici, C. Turchetti, and P. Crippa, "Multicomponent AM–FM demodulation: the state of the art after the development of the iterated Hilbert transform," in *Proc. Int. Conf. Sig. Process. Commun.*, Nov. 2007, pp. 1471–1474.

[50] Z. Feng, D. Zhang, and M. J. Zuo, "Adaptive mode decomposition methods and their applications in signal analysis for machinery fault diagnosis: a review with examples," *IEEE Access*, vol. 5, pp. 24 301–24 331, 2017.

[51] D. E. Vakman and L. A. Vainshtein, "Amplitude, phase, frequency–fundamental concepts in the theory of oscillations," *Uspekhi Fizicheskikh Nauk*, vol. 123, pp. 657–682, 1977.

[52] M. Feldman, "Non-linear system vibration analysis using Hilbert transform–I. Free vibration analysis method 'FREEVIB'," *Mech. Syst. and Signal Process.*, vol. 8, no. 2, pp. 119–127, Mar. 1994.

[53] A. Rao and R. Kumaresan, "On decomposing speech into modulated components," *IEEE Trans. Speech Audio Process.*, vol. 8, no. 3, pp. 240–254, May 2000.

[54] F. Gianfelici, G. Biagetti, P. Crippa, and C. Turchetti, "Multicomponent AM–FM representations: an asymptotically exact approach," *IEEE Trans. Audio Speech Lang. Process.*, vol. 15, no. 3, pp. 823–837, Mar. 2007.

[55] M. Feldman, "Theoretical analysis and comparison of the Hilbert transform decomposition methods," *Mech. Syst. and Signal Process.*, vol. 22, no. 3, pp. 509–519, Apr. 2008.

[56] ——, *Hilbert Transform Applications in Mechanical Vibration*. Wiley, 2011.

[57] P. Maragos, J. F. Kaiser, and T. F. Quatieri, "Energy separation in signal modulations with application to speech analysis," *IEEE Trans. Signal Process.*, vol. 41, no. 10, pp. 3024–3051, Oct. 1993.

[58] A. C. Bovik, P. Maragos, and T. F. Quatieri, "AM–FM energy detection and separation in noise using multiband energy operators," *IEEE Trans. Signal Process.*, vol. 41, no. 12, pp. 3245–3265, Dec. 1993.

[59] A. Potamianos and P. Maragos, "A comparison of the energy operator and the Hilbert transform approach to signal and speech demodulation," *Signal Process.*, vol. 37, no. 1, pp. 95–120, 1994.

[60] L. B. Fertig and J. H. McClellan, "Instantaneous frequency estimation using linear prediction with comparisons to the DESAs," *IEEE Signal Process. Lett.*, vol. 3, no. 2, pp. 54–56, Feb. 1996.

[61] A. Potamianos and P. Maragos, "Speech analysis and synthesis using an AM–FM modulation model," *Speech Commun.*, vol. 28, no. 3, pp. 195–209, July 1999.

[62] T. F. Quatieri, *Discrete-Time Speech Signal Processing*. Prentice Hall, 2002.

[63] A. O. Boudraa, J. C. Cexus, F. Salzenstein, and L. Guillon, "IF estimation using empirical mode decomposition and nonlinear Teager energy operator," in *Int. Symp. Cont., Comm. Sig. Process.*, 2004, pp. 45–48.

[64] E. S. Diop, A. O. Boudraa, and F. Salzenstein, "A joint 2D AM–FM estimation based on higher order Teager–Kaiser energy operators," *Signal, Image and Video Process.*, vol. 5, no. 1, pp. 61–68, 2011.

[65] P. Rao and F. J. Taylor, "Estimation of instantaneous frequency using the discrete Wigner distribution," *Electron. Lett.*, vol. 26, no. 4, pp. 246–248, Feb. 1990.

[66] Y. Pantazis, O. Rosec, and Y. Stylianou, "Adaptive AM–FM signal decomposition with application to speech analysis," *IEEE Trans. Audio Speech Lang. Process.*, vol. 19, no. 2, pp. 290–300, Feb. 2011.

[67] B. Boashash, G. Azemi, and J. O'Toole, "Time-frequency processing of nonstationary signals: advanced TFD design to aid diagnosis with highlights from medical applications," *IEEE Signal Process. Mag.*, vol. 30, no. 6, pp. 108–119, Nov. 2013.
[68] J. Gilles, "Empirical wavelet transform," *IEEE Trans. Sig. Proc.*, vol. 61, no. 16, pp. 3999–4010, 2013.
[69] H. T. Wu, P. Flandrin, and I. Daubechies, "One or two frequencies? the synchrosqueezing answers," *Adv. Adapt. Data Anal.*, vol. 3, no. 01n02, pp. 29–39, 2011.
[70] Z. Wu and N. E. Huang, "Ensemble empirical mode decomposition: a noise-assisted data analysis method," *Adv. Adapt. Data Anal.*, vol. 1, no. 01, pp. 1–41, 2009.
[71] S. Sandoval and P. L. De Leon, "Advances in empirical mode decomposition for computing instantaneous amplitudes and instantaneous frequencies," in *Proc. IEEE Int. Conf. Acoust. Speech Signal Process.*, Mar. 2017.
[72] S. Meignen and V. Perrier, "A new formulation for empirical mode decomposition based on constrained optimization," *IEEE Signal Process. Lett.*, vol. 14, no. 12, pp. 932–935, 2007.
[73] Y. Kopsinis and S. McLaughlin, "Investigation and performance enhancement of the empirical mode decomposition method based on a heuristic search optimization approach," *IEEE Trans. Signal Process.*, vol. 56, no. 1, pp. 1–13, 2008.
[74] T. Y. Hou and Z. Shi, "Data-driven time–frequency analysis," *Appl. Comput. Harmonic Anal.*, vol. 35, no. 2, pp. 284–308, 2013.
[75] D. Looney and D. P. Mandic, "A machine learning enhanced empirical mode decomposition," in *Proc. IEEE Int. Conf. Acoust. Speech Signal Process.*, 2008, pp. 1897–1900.
[76] E. Deléchelle, J. Lemoine, and O. Niang, "Empirical mode decomposition: an analytical approach for sifting process," *IEEE Signal Process. Lett.*, vol. 12, no. 11, pp. 764–767, 2005.
[77] R. Sharpley and V. Vatchev, "Analysis of the intrinsic mode functions," *Constr. Approx.*, vol. 24, no. 1, pp. 17–47, 2006.
[78] V. Vatchev and R. Sharpley, "Decomposition of functions into pairs of intrinsic mode functions," *Proc. R. Soc. Lond. A Math. Phys. Sci.*, vol. 464, no. 2097, pp. 2265–2280, 2008.
[79] E. H. Diop, R. Alexandre, and A. O. Boudraa, "A PDE characterization of the intrinsic mode functions," in *Proc. IEEE Int. Conf. Acoust. Speech Signal Process.*, 2009, pp. 3429–3432.
[80] E. S. Diop, R. Alexandre, and A. O. Boudraa, "Analysis of intrinsic mode functions: a PDE approach," *IEEE Signal Process. Lett.*, vol. 17, no. 4, pp. 398–401, 2010.
[81] S. D. E. Hadji, R. Alexandre, and V. Perrier, "A PDE based and interpolation-free framework for modeling the sifting process in a continuous domain," *Adv. Comput. Math.*, vol. 38, no. 4, pp. 801–835, 2013.
[82] Y. Tang, D. Gao, and G. Lup, "Non-linear bearing force of the rolling ball bearing and its influence on vibration of bearing system," *J. Aerospace Power*, vol. 2, p. 024, 2006.
[83] Q. Du and S. Yang, "Application of the EMD method in the vibration analysis of ball bearings," *Mechanical Systems and Signal Processing*, vol. 21, no. 6, pp. 2634–2644, 2007.
[84] L. Lin, Y. Wang, and H. Zhou, "Iterative filtering as an alternative algorithm for empirical mode decomposition," *Adv. Adapt. Data Anal.*, vol. 1, no. 04, pp. 543–560, 2009.
[85] A. Cicone, J. Liu, and H. Zhou, "Adaptive local iterative filtering for signal decomposition and instantaneous frequency analysis," *Appl. Comput. Harmonic Anal.*, vol. 41, no. 2, pp. 384–411, 2016.
[86] O. Niang, E. Deléchelle, and J. Lemoine, "A spectral approach for sifting process in empirical mode decomposition," *IEEE Trans. Signal Process.*, vol. 58, no. 11, pp. 5612–5623, 2010.
[87] G. Rilling, P. Flandrin, P. Gonçalves, and J. M. Lilly, "Bivariate empirical mode decomposition," *IEEE Signal Process. Lett.*, vol. 14, no. 12, pp. 936–939, 2007.
[88] T. Tanaka and D. P. Mandic, "Complex empirical mode decomposition," *IEEE Signal Process. Lett.*, vol. 14, no. 2, pp. 101–104, 2007.
[89] N. Rehman and D. P. Mandic, "Multivariate empirical mode decomposition," in *Proc. R. Soc. Lond. A Math. Phys. Sci.*, vol. 466, no. 2117, 2010, pp. 1291–1302.
[90] J. Fleureau, J. Nunes, A. Kachenoura, L. Albera, and L. Senhadji, "Turning tangent empirical mode decomposition: a framework for mono-and multivariate signals," *IEEE Trans. Signal Process.*, vol. 59, no. 3, pp. 1309–1316, 2011.
[91] A. Ahrabian, N. Rehman, and D. P. Mandic, "Bivariate empirical mode decomposition for unbalanced real-world signals," *IEEE Sig. Proc. Lett.*, vol. 20, no. 3, pp. 245–248, 2013.
[92] D. P. Mandic, N. Rehman, W. Zhaohua, and N. E. Huang, "Empirical mode decomposition-based time-frequency analysis of multivariate signals: the power of adaptive data analysis," *IEEE Signal Process. Mag.*, vol. 30, no. 6, pp. 74–86, Nov. 2013.
[93] C. Damerval, S. Meignen, and V. Perrier, "A fast algorithm for bidimensional EMD," *IEEE Signal Process. Lett.*, vol. 12, no. 10, pp. 701–704, 2005.
[94] Z. Wu, N. E. Huang, and X. Chen, "The multi-dimensional ensemble empirical mode decomposition method," *Adv. Adapt. Data Anal.*, vol. 1, no. 03, pp. 339–372, 2009.
[95] A. Linderhed, "Image empirical mode decomposition: a new tool for image processing," *Adv. Adapt. Data Anal.*, vol. 1, no. 02, pp. 265–294, 2009.
[96] D. P. Mandic and N. Rehman, "Filter bank property of multivariate empirical mode decomposition," *IEEE Trans. Signal Process.*, vol. 59, no. 5, pp. 2421–2426, 2011.
[97] J. C. Nunes and E. Deléchelle, "Empirical mode decomposition: applications on signal and image processing," *Adv. Adapt. Data Anal.*, vol. 1, no. 01, pp. 125–175, 2009.
[98] M. G. Frei and I. Osorio, "Intrinsic time-scale decomposition: time–frequency–energy analysis and real-time filtering of non-stationary signals," in *Proc. R. Soc. Lond. A*, vol. 463, no. 2078, 2007, pp. 321–342.
[99] S. Chen, X. Dong, Z. Peng, W. Zhang, and G. Meng, "Nonlinear chirp mode decomposition: a variational method," *IEEE Trans. Signal Process.*, vol. 65, no. 22, pp. 6024–6037, 2017.
[100] J. S. Smith, "The local mean decomposition and its application to EEG perception data," *J. R. Soc. Interface*, vol. 2, no. 5, pp. 443–454, 2005.
[101] D. Iatsenko, P. V. McClintock, and A. Stefanovska, "Nonlinear mode decomposition: a noise-robust, adaptive decomposition method," *Phys. Rev. E*, vol. 92, no. 3, p. 032916, 2015.
[102] J. Zheng, J. Cheng, and Y. Yang, "A rolling bearing fault diagnosis approach based on LCD and fuzzy entropy," *Mechanism and Machine Theory*, vol. 70, pp. 441–453, 2013.

BIOGRAPHY

Steven Sandoval received the B.S. Electrical Engineering and M.S. Electrical Engineering from New Mexico State University in 2007 and 2010 respectively, and the Ph.D. degree in Electrical Engineering from Arizona State University in 2016. Currently, he is at the Klipsch School of Electrical and Computer Engineering at New Mexico State University. His research interests include audio and speech processing, time-frequency analysis, and machine learning.

Phillip L. De Leon (SM'03) received the B.S. Electrical Engineering and the B.A. in Mathematics from the University of Texas at Austin, in 1989 and 1990 respectively and the M.S. and Ph.D. degrees in Electrical Engineering from the University of Colorado at Boulder, in 1992 and 1995 respectively. Currently, he serves as Associate Dean of Research in the College of Engineering and is a Professor in the Klipsch School of Electrical and Computer Engineering at New Mexico State University. His research interests include audio and speech processing, machine learning, and time-frequency analysis.